University of Nevada, Reno

Instantaneous Electric Power as a Tool for Control of Induction Motors – A Pilot Study

A thesis submitted in partial fulfillment
of the requirements for the degree of

MASTER OF SCIENCE IN ELECTRICAL ENGINEERING

by

FEN NIU

Dr. Andrzej M. Trzynadlowski, Thesis Advisor

August, 2012

THE GRADUATE SCHOOL

We recommend that the thesis
prepared under our supervision by

FEN NIU

entitled

**Instantaneous Electric Power as a Tool for Control of Induction Motors - A Pilot
Study**

be accepted in partial fulfillment of the
requirements for the degree of

MASTER OF SCIENCE

Andrzej M. Trzynadlowski, Advisor

M. Sami Fadali, Committee Member

Paula Noble, Graduate School Representative

Marsha H. Read, Ph. D., Dean, Graduate School

August, 2012

ABSTRACT

The thesis is devoted to the concept of direct power control as a tool for control of induction motors. Power distribution in the induction motor is analyzed using both the exact and simplified models of the motor. An improved sensorless Instantaneous Power Control (IPC) technique based on the known IPC method is also proposed. Computer simulations are presented for confirmation of the theoretical conclusions.

Following power analysis of a simplified model of the induction motor, it is shown that the motor torque can be controlled by adjusting the input active power. The magnetic flux can be controlled by adjusting the stator current by selecting a suitable voltage space vector at the beginning of each switching interval. We named that idea as Direct Power Control (DPC), it may facilitate development of novel control methods of induction motor in future studies.

It has also has been found that the IPC requires that the magnetic flux be generated first employing the direct torque control (DTC). Except for this limitation, the novel sensorless IPC displays a good dynamic response.

Keywords: Induction motor, Direct Power Control (DPC), Instantaneous Power Control (IPC), voltage source inverter, instantaneous active and reactive powers, Direct Torque Control (DTC).

ACKNOWLEDGEMENT

Graduate study at the University of Nevada, Reno brought experience and knowledge to both my life and study. I would like to thank my advisor, Dr. Andrezej M. Trzynadlowski, for his support during the past two years. His patience and enthusiasm influenced me to work towards my goals.

I would also like to thank Dr. Sami Fadali, for his generous help in and out of his classes.

I also want to express my gratitude to Dr. Paula Noble, for accepting my request to be a member of my graduate committee.

Finally, I want to thank my family – my mom and sister, for their selfless support.

TABLE OF CONTENTS

LIST OF TABLES

LIST OF FIGURES

LIST OF SYMBOLS

R_s Stator resistance

R_r Rotor resistance

L_s Stator inductance

L_r Rotor inductance

L_{ls} Stator leakage inductance

L_{lr} Rotor leakage inductance

V_s Stator voltage

ω_s Synchronous speed

ω_r Rotor electrical speed

ω_m Rotor mechanical speed

ω_{sl} Electrical slip speed

λ_s Stator flux

λ_r Rotor flux

θ_s Stator flux angle

θ_r Rotor flux angle

P_p Number of pole pairs

V_{dc} DC supply voltage for voltage source inverter

J Rotor mass moment of inertia

T_{load} Load torque

T_e Electromagnetic torque

P_{in} Input active power

P_{total} Total active power

P_{out} Output active power

P_{mech} Mechanical power

P_R Active power consumed by resistance

P_L Active power related to an inductance

p_m Active power related to magnetizing inductance

Q_{in} Input average reactive power

Q_{total} Total average reactive power

q_m Reactive power related to magnetizing inductance

CHAPTER 1

INTRODUCTION

The induction motor converts electrical power into mechanical power. In variable speed drives (VSD), the induction motor represents a source of torque. As such, it is employed as an actuator in speed- and position-control electromechanical systems. Two control techniques dominate the technology of VSDs: the field-orientation control (FOC) and direct torque control (DTC). The FOC system controls the stator current, while a DTC system controls the stator voltage. More precisely, the DTC consists in selecting consecutive states of the voltage-source inverter supplying the motor. In both systems, the input voltage and current are also sources of information about the dynamic state of the machine, especially in the so-called sensorless drives. Those drives lack sensors of non-electrical quantities, such as the speed, position, or magnetic flux.

Knowledge of the stator current and state of the inverter allows easy computation of the instantaneous complex electric power, which in multi-phase systems has both the real, p, and reactive, q, components. In power electronic converters, the p and q signals have been extensively used as control tools. For example, driving q to zero results in the desirable unity input power factor of ac-ac and ac-dc converters. In contrast, apart from a few papers by Betz and his collaborators (see Chapter 2 for literature review), the issue of instantaneous electric power has been almost absent from the vast technical literature on induction motor drives.

The lack of follow-up on Betz's work seems to indicate some serious problems with the implementation of his ideas. This pilot study does not aim at a development of a complete "direct power control" strategy. Instead, relations between the torque and flux of the induction motor and the instantaneous active and reactive input powers are examined. Assuming that within a single switching/sampling cycle the current does not change significantly, the values of p and q can be predicted for each next state of the inverter. The question is whether they can be used for a selection of the state resulting in the best dynamic performance of the motor and how can that be done.

The difficulty with dealing with instantaneous powers is that p is not only transferred to the load and dissipated in the motor resistances but that it also enters and leaves the inductances of the machine. The average real power in an inductance is zero, but it is not so with the instantaneous power. Also, a physical interpretation of instantaneous reactive power is difficult. It can only be defined for multi-phase systems, which leads to the explanation that it represents as zero-balance power exchange between phases. On the other hand, if the motor did not have inductances, it would not need reactive power, but also no magnetic flux necessary for its operation could be produced.

Although an analysis of the mathematical model of the motor could answer some important questions, the practical control method should not rely too much on that model. Both the resistances and inductances of the machine change with the operating conditions due to such phenomena as temperature impacts, skin effects, or magnetic saturation. Therefore, some simplified, heuristic rules have been sought to assess how p and q affect the torque and flux of the motor. Numerous computer simulations have been performed for that purpose, and certain general observations have been made.

The thesis is structured as follows. Chapter 2 contains a literature review as a background of the project. The mathematical model of the induction motor is presented in Chapter 3. Chapter 4 describes the classic DTC, Direct Input Power and Flux Control (DIPC), and Direct Output Power and Flux Control (DOPC) methods. They are related to the idea of instantaneous powers as a tool for the control of induction motor explored in this research, as the DTC, DIPC, DOPC and the envisioned DPC consist in selecting the next inverter state. The concept of instantaneous complex power and its d and q components is expounded in Chapter 5. The power distribution using both an exact and a simplified model of the induction motor is analyzed and relevant simulations are presented. A sensorless IPC technique for induction motors is proposed in Chapter 6. Chapter 7 concludes the work.

CHAPTER 2

LITERATURE REVIEW

Induction motors play a dominant role in industry thanks to their advantages – robustness, low price, and easy maintenance. In recent decades, control techniques of induction motor have attracted researchers' attention. Induction motor control methods can be classified as scalar control based on the constant volts-per-hertz (CVH) principle, vector control based on the field orientation (direct and indirect), and direct torque control (DTC). The scalar control is usually employed in low-performance drives, while field orientation is used in high-performance drives, such as positioning ones.

DTC was proposed in 1990s and still hundreds of papers are presented every year to improve drive performance with respect to the torque ripple and limited speed range. The subsequent section, the most common control techniques will be briefly described.

2.1 Field Oriented Control of Induction Machines

The field oriented control (FOC) contains two classes depending on the method of obtaining the machine flux information. They are the Direct and Indirect Flux Orientation (DFO and IFO). Three major fluxes in the induction motor are the stator flux, the air-gap flux, and the rotor flux.

The air-gap magnetic field can be easily measured by Hall sensors. The direct rotor flux orientation estimates the rotor flux's magnitude and angular position from measured air-gap flux and the relationship between air-gap and rotor flux. Also, we can calculate the

rotor flux from stator flux taking the advantage of their relationship through stator leakage, main inductance and rotor leakage. First we need to estimate the stator flux by using stator voltage and current. Instead of using flux sensors in DFO drives, the IFO employs measurement of the rotor position to estimate the rotor flux. The rotor flux and developed torque in IFO drives are controlled in a feed-forward manner, i.e., no feedback loops are employed. As a result, the indirect rotor flux orientation systems are less robust than those employing the direct method [1].

Rotor flux depends on the rotor inductance, especially the leakage part. It has been reported that for a standard induction machine with closed rotor slots the conventional no-load or short-circuit tests cannot give the correct values for machine inductances. It has also been observed that due to the closed rotor slots, the inductance varies with operating conditions [2]-[3], so the estimation error of rotor flux is unavoidable, which further influences the induction machines' dynamic performance.

Stator flux is dependent on the stator resistance that can be measured accurately in most cases. Therefore, control schemes based on stator flux instead of rotor flux have been developed. Compared with rotor flux oriented vector control, stator flux oriented control is somewhat more complex, but direct and indirect control methods in terms of stator flux orientation are quite common in practice. Air-gap magnetic field must be measured both in the stator and rotor flux oriented vector control, if the direct method is used.

The common goal in the field oriented vector control methods for induction motors is to decouple the stator current into a torque current component and a flux current

component. This allows controlling the electromagnetic torque and flux separately. To some degree, FOC makes the induction motor work like a DC motor. In 1988, the idea of the UFO (Universal Field Oriented) Controller that decouples flux and torque in an arbitrary flux reference frame was proposed [6]. Thanks to its high degree of generality the UFO controller lends itself to be fully compatible with all existing field oriented controllers, indirect as well as direct field orientation. Scholars also suggested that different reference frames can be adopted for low speed and high speed regions respectively [7]-[10]. However the field orientation methods suffer from specific problems. The changing load and temperature influence the rotor parameters in the DFO systems. The IFO method is less sensitive to rotor parameters at the expense of difficult flux measurement at zero frequency.

Hall sensors of magnetic flux are seldom used in practice, so the flux is usually estimated from the terminal variables, using a mathematical model of the motor. Specifically, the relationship between stator/air-gap flux and rotor flux through stator and rotor leakage and main inductance are employed [11]. Analyzing the advantages and disadvantages of UFO in different reference frames, [11] showed that although an improved UFO can enhance the dynamic performance and reduce the influence of motor parameters, the control system becomes quite complex. The designer needs to find the best tradeoff between system's complexity and performance.

2.2 Direct Torque Control of Induction Machines

Considering the disadvantages of FOC – coordinate transformation and sensitivity to motor parameters. Takahashi and Noguchi proposed the DTC of induction motor for low and medium power applications [12]. Later, DTC for high power application, the so-

called direct self-control (DSC) was developed by Depenbrock [13]. Compared with FOC, DTC directly selects the new state of the inverter feeding the motor. It improves the system dynamic response and the control system is quite simple. However, DTC's performance deteriorates at low speeds, and the current ripple is usually higher than in a comparable FOC drive. The current ripple causes torque ripple, generates noise and vibration, and produces errors in sensorless drives. Due to the variable switching frequency, high sampling rates are needed to implement the hysteresis control of torque and flux.

The reason why torque and current ripples exist is that during most of a switching period no exact voltage vectors to produce the desired torque and flux can be provided. An inverter can only produce six active and two zero vectors. This limitation motivated development of improved DTC methods, such as the space-vector modulation DTC (SVM-DTC) and direct SVM-DTC (DSVM-DTC). In SVM-DTC, the required voltage space vector to compensate the flux and torque errors is calculated using a predictive technique [14]. There are various SVM techniques, such as the Direct-Reverse SVM, Direct-Direct SVM, Direct-Direct with Vnull = [000], Direct-Direct with Vnull = [111] [15]. The choice of SVM technique depends on the optimization criteria under consideration, whether it is the torque/current ripple, the harmonic losses or the switching losses [16]-[17].

Another method to improve DTC involves use of a multilevel inverter. If a three-level inverter replaces the conventional two-level inverter a much greater number of voltage space vectors can be generated, with less harmonic distortion and lower switching frequency. However, the cost of such a system is higher than that of one based on a

standard inverter [18-21]. Combining DTC with intelligent control methods, such as fuzzy-logic control, improves the dynamic response of a DTC drive [22]-[23].

A fuzzy-logic based duty ratio controller determines the duty ratio of the active voltage vector in each switching period as a nonlinear function of torque error, flux error and flux position [24]-[27]. This can reduce the torque ripple to less than 1/3 of the conventional DTC [24]. Reference [28] proposes a method that combines the SVM-PWM with a fuzzy-logic controller, which generates the reference voltage space vector in each switching period. A look-up table that indicates the most appropriate torque-increasing vector to apply is described in [29].

2.3 Instantaneous Power Control of Induction Machines

The IPC (Instantaneous Power Control) of induction motors was proposed and expanded by Betz in [31]-[37]. The reference active and reactive powers are produced in a control system based on the air-gap flux oriented synchronous frame. The technique lies somewhere between the DTC and FOC. The advantages of IPC include its simple control algorithm, robustness, and limited dependence on detailed knowledge of parameters. Although this method can decouple controls of the torque and flux, the quality of flux control is low, especially when the reference speed is very high or very low. The IPC idea has been utilized in the control of an induction motor fed by a three-phase matrix converter [38]-[39].

2.4 Direct Power Control of PWM Rectifiers

It is worth mentioning that the direct power control (DPC) has been successfully employed in PWM rectifiers. Publications [41]-[43] show that the DPC of a three phase PWM rectifier has distinct advantages in comparison with the traditional voltage-oriented control (VOC). The so-called virtual-flux based DPC (VF-DPC) has a simple algorithm and is less sensitive to unbalanced supply voltage. Introducing the SVM allows reduction of the high switching frequency [45]-[46]. Note that when a three phase rectifier is analyzed, it can be regarded as formally similar to a three phase synchronous generator. This may indicate the possibility of applying the VF-DPC to permanent-magnet synchronous generators.

CHAPTER 3

MATHEMATICAL MODEL OF THE INDUCTION MOTOR

Development of modern power electronics during the past half century significantly enhanced electromechanical power conversion systems, such as electric motor drives. Rectifiers and inverters are necessary components of adjustable speed induction motor drives, converting the raw power to that with controlled ac voltage of the required magnitude and frequency. In this chapter, fundamental relations of the inverter, the concept of space vectors, coordinate transformation, and the mathematical model of the induction motor are described.

3.1 Voltage Space Vectors

To simplify the dynamic model of the three-phase induction motor, the concept of space vectors was introduced by GE researchers in the nineteen twenties. The three magnetomotive forces produced by three phase stator currents are combined into a single space vector that rotates with an angular velocity depending on the supply radian frequency and number of magnetic poles. This idea can be extended on the current, voltage, and magnetic flux. Unlike phasors used in the steady-state analysis of ac circuits, including that of the induction motor, vectors are applicable to both sinusoidal and non-sinusoidal electrical variables. This greatly facilitates the analysis of transient phenomena in electric machines.

The voltage space vector $\vec{v}$ is defined as,

$$\vec{v} = \vec{v_a} + \vec{v_b} + \vec{v_c} = v_a + v_b e^{j\frac{2\pi}{3}} + v_c e^{j\frac{4\pi}{3}} \tag{3.1}$$

In a three-wire three-phase system, the sum of three phase voltages is zero, that is, $v_a + v_b + v_c = 0$. Thus, two of these three voltages are independent. Consequently, a three-phase system can be transformed to an equivalent two-phase system in a set of coordinates, subsequently referred to as a stationary reference frame, as illustrated in Figure 3.1.
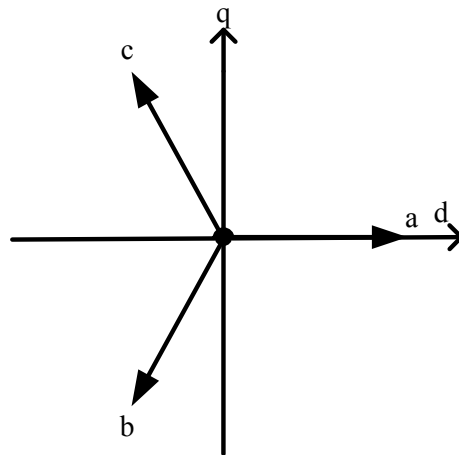
Fig. 3.1 Transformation from three-phases coordinates to two phase stationary coordinates.

The three-phase (*abc*) to two-phase (*dq*) conversion is described by the Park transformation.

$$\begin{bmatrix} v_d \\ v_q \end{bmatrix} = \begin{bmatrix} 1 & -\frac{1}{2} & -\frac{1}{2} \\ 0 & \frac{\sqrt{3}}{2} & -\frac{\sqrt{3}}{2} \end{bmatrix} \begin{bmatrix} v_a \\ v_b \\ v_c \end{bmatrix} \tag{3.2}$$

An alternative version of the Park transformation has a coefficient of 2/3 on the right-hand side of Equation (3.2), to make each vector magnitude equal to the peak value of

the corresponding phasor. This difference of coefficients is of little importance as it does not affect motor performance, but it may yield incorrect numerical results when forgotten about. For example, if we choose Equation (3.2), the magnitude of voltage vector is 1.5 times greater than the peak value of a single phase voltage and $1.5\sqrt{2}$ times greater than its RMS value.

The complex power in a three-phase balanced sinusoidal system can be expressed as

$$\bar{S}_{abc} = 3\bar{V}_{ph}\bar{I}_{ph}^{*} \tag{3.3}$$

where $\bar{V}_{ph}$ and $\bar{I}_{ph}$ are the rms phasors of phase voltage and current, respectively, and the superscript "*" denotes a conjugate phasor. In the *d-q* coordinates, complex power is given by

$$S_{dq} = \vec{V_S}\,\vec{I_S}^{*} \tag{3.4}$$

where $\vec{V_S}$, $\vec{I_S}$ represent the stator voltage and current vectors. As

$$V_S = 1.5\sqrt{2}\,V_{ph} \tag{3.5}$$

$$I_S = 1.5\sqrt{2}\,I_{ph} \tag{3.6}$$

then

$$S_{dq} = 1.5\sqrt{2}\,V_{ph} * 1.5\sqrt{2}\,I_{ph}^{*} = 4.5V_{ph}I_{ph}^{*} \tag{3.7}$$

Comparing Equations (3.3) and (3.7) we see that the magnitudes of the powers in different reference frames are not equal. Thus we need a coefficient K to balance them. If we choose K = 2/3, then

$$S_{abc} = K\, S_{dq} = \frac{2}{3}\, S_{dq} \tag{3.8}$$

and, $S_{abc} = S$ can be expressed as,

$$\vec{S} = \frac{2}{3}\vec{V_S}\,\vec{I_S}^* \tag{3.9}$$

3.2 Three-Phase Voltage-Source Inverter

The application of voltage space vectors facilitates the control of the three-phase voltage-source inverter which is the most common converter in adjustable speed ac drives with induction motors. Its diagram is shown in Figure 3.2. The upper switches are denoted by SA, SB, and SC, and the lower ones by SA', SB', and SC'. We define the switching variable *a* as equal to 1, if SA is on and SA' is off, while *a* = 0 when SA is off and SA' is on. Similarly, switching variables *b* and *c* are defined for the remaining two legs of the inverter.
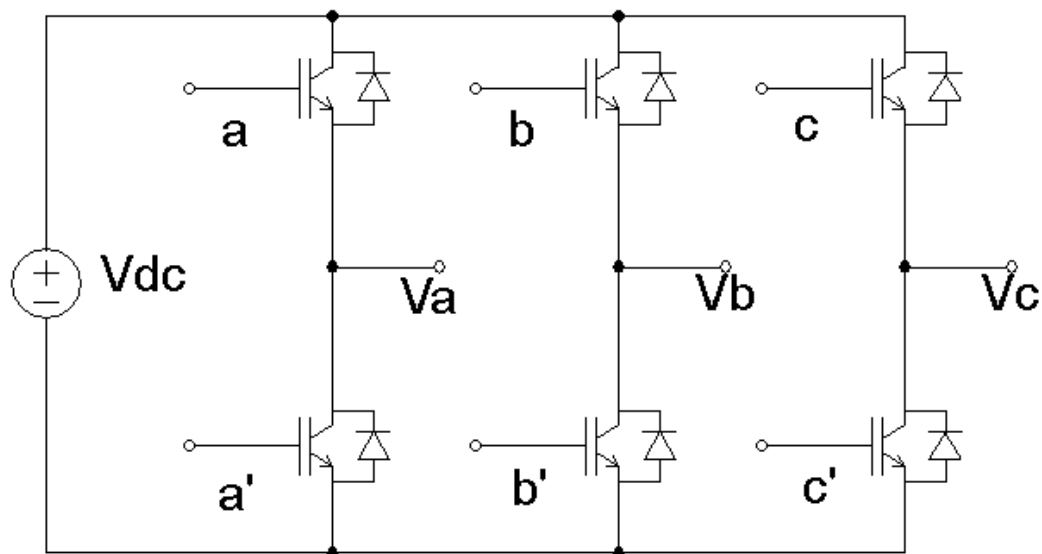
Fig. 3.2 Power circuit diagram of a three-phase voltage source inverter.

Considering that two switches in the same leg cannot be turned on or off at the same time, we have a total of 8 possible states, which include six active states and two zero states. The line-to-neutral output voltages of the inverter are given by,

$$V_{AN} = \frac{1}{3}V_i(2a - b - c) \tag{3.10}$$

$$V_{BN} = \frac{1}{3}V_i(2b - a - c) \tag{3.11}$$

$$V_{CN} = \frac{1}{3}V_i(2c - b - a) \tag{3.12}$$

and the corresponding voltage vector is,

$$\begin{bmatrix} v_d \\ v_q \end{bmatrix} = V_i \begin{bmatrix} 1 & -\frac{1}{2} & -\frac{1}{2} \\ 0 & \frac{\sqrt{3}}{2} & -\frac{\sqrt{3}}{2} \end{bmatrix} \begin{bmatrix} a \\ b \\ c \end{bmatrix} \tag{3.13}$$

Table 3.1 shows the d-q voltage component for each switching state.

Table 3.1. Voltage space vectors for individual states of the inverter

a	b	c	100	110	010	011	001	101	000	111
	v_d		V_i	$\frac{1}{2}V_i$	$-\frac{1}{2}V_i$	$-V_i$	$-\frac{1}{2}V_i$	$\frac{1}{2}V_i$	0	0
	v_q		0	$\frac{\sqrt{3}}{2}V_i$	$\frac{\sqrt{3}}{2}V_i$	0	$-\frac{\sqrt{3}}{2}V_i$	$\frac{1}{2}V_i$	0	0

The six non-zero voltage vectors are shown in Figure 3.3. The magnitude of each vector is equal to the input dc voltage of the inverter. Two adjacent vectors frame a 60° sector (sextant). The zero vectors are in the origin.
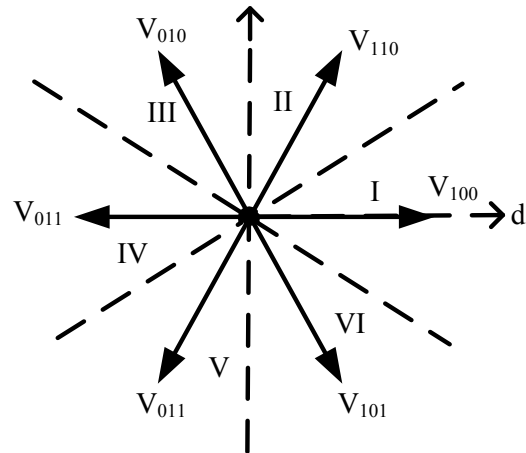
Fig. 3.3. Voltage space vectors of the inverter.

Here for the convenience of DTC analysis in Chapter 4, we define six sectors for Figure 3.3 as follows,

Table 3.2. Definition of sectors

Sector	Angle range /°
I	[-30, 30]
II	[30, 90]
III	[90,150]
IV	[150, -150]
V	[-150, -90]
VI	[-90, -30]

3.3 Induction Motor

The induction motor comprises a stator and a rotor mounted on mechanical bearings and separated from the stator by an air gap [47]. Nowadays induction motors are the most popular machine used in industry. Before discussing control issues, the mathematic model of the induction motor is presented.

The induction motor's electrical model can be viewed as an assembly of inductances, resistances, and a voltage source on the rotor side. For the three-phase induction motor, there are six circuits/phases, three in the stator and three in the rotor. The following equations describe the induction motor in the three-phase stationary reference frame.

$$[V] = [r][i] + [L]\frac{d[i]}{dt} + \frac{d[L]}{d\theta_{er}}[i]\frac{d\theta_{er}}{dt} \tag{3.14}$$

$$T_e = \frac{1}{2}\, p_p\, [i]^T\, \frac{d[L]}{d\theta_{er}}\, [i] \tag{3.15}$$

$$T_e - T_l = \frac{J}{p_p}\frac{dw_r}{dt} \tag{3.16}$$

where

$$[V] = [V_a, V_b, V_c, V_{ar}, V_{br}, V_{cr}]^T$$

$$[i] = [i_a, i_b, i_c, i_{ar}, i_{br}, i_{cr}]^T$$

$$[L] = \left[L_{a,b,c,a_r,b_r,c_r}(\theta_{er})\right]$$

$$[r] = Diag[r_s, r_s, r_s, r_r, r_r, r_r]$$

The inductance matrix [L] changes with time, which complicates the analysis of induction motor. Fortunately, Equations (3.14)-(3.16) can be transformed to an arbitrary reference frame that rotates with the speed w_b using space vectors. The transformation yields

$$\overrightarrow{V_s} = R_s\overrightarrow{I_s} + \frac{\overrightarrow{d\lambda_s}}{dt} + j\omega_b\overrightarrow{\lambda_s} \tag{3.17}$$

$$0 = R_r\overrightarrow{I_r} + \frac{\overrightarrow{d\lambda_r}}{dt} + j(\omega_b - \omega_r)\overrightarrow{\lambda_r} \tag{3.18}$$

$$\frac{J}{P_p}\frac{d\omega_r}{dt} = T_e - T_l \tag{3.19}$$

$$T_e = \frac{2}{3}pp(\lambda_{sd}i_{sq} - \lambda_{sq}i_{sd}) \tag{3.20}$$

$$\overrightarrow{\lambda_s} = L_s\overrightarrow{I_s} + L_m\overrightarrow{I_r} \tag{3.21}$$

$$\overrightarrow{\lambda_r} = L_r\overrightarrow{I_r} + L_m\overrightarrow{I_s} \tag{3.22}$$

where,

$\overrightarrow{V_s}$ is the stator voltage space vector

$$\overrightarrow{V_s} = V_{sd} + jV_{sq} \tag{3.23}$$

$\overrightarrow{I_s}, \overrightarrow{I_r}$ are the stator and rotor current space vectors

$$\overrightarrow{I_s} = i_{sd} + ji_{sq} \tag{3.24}$$

$$\overrightarrow{I_r} = i_{rd} + ji_{rq} \tag{3.25}$$

$$\overrightarrow{\lambda_s} = \lambda_{sd} + j\lambda_{sq} \tag{3.26}$$

$$\vec{\lambda_r} = \lambda_{rd} + j\lambda_{rq} \tag{3.27}$$

$$L_s = L_m + L_{s\sigma} \tag{3.28}$$

$$L_r = L_m + L_{r\sigma} \tag{3.29}$$

L_s , L_r are the stator and rotor inductances

$L_{s\sigma}$ is the stator leakage inductance

L_m is the magnetizing inductance

$L_{r\sigma}$ is the rotor leakage inductance

If $\omega_b = 0$, which means a stationary reference frame, the dynamic equations of induction motor become

$$\vec{V_s} = R_s\vec{I_s} + \frac{d\vec{\lambda_s}}{dt} \tag{3.30}$$

$$0 = R_r\vec{I_r} + \frac{d\vec{\lambda_r}}{dt} - j\omega_r\vec{\lambda_r} \tag{3.31}$$

while the torque equation is unchanged. In this case, we have the equivalent circuit for the induction motor as shown in Figure 3.4.
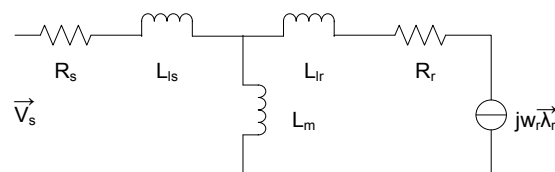

Fig. 3.4 Equivalent circuit of induction motor in the stationary reference frame.

If we ignore the stator resistance, which is usually small when compared with the stator leakage reactance, the motor model consists of three inductors, one resistor and a voltage source. The Γ model is particularly convenient for an analysis of the induction motor.

In addition to the stationary reference frame, we define a frame rotating at an angular speed of ω_e, $\omega_e = \frac{d\theta}{dt}$. The stator voltage vector $\overrightarrow{V_e}$ in the rotating frame is given by

$$\overrightarrow{V_e} = \overrightarrow{v_s} e^{-j\theta_e} \tag{3.32}$$

where

$$e^{-j\theta_e} = \cos(\theta_e) + j\sin(\theta_e) \tag{3.33}$$

If D and Q denote the real and imaginary components of a vector in the rotating frame, as opposed to d and q in the stationary frame, then the transformation between these frames is described by

$$\begin{bmatrix} v_D \\ v_Q \end{bmatrix} = \begin{bmatrix} \cos(\theta_e) & \sin(\theta_e) \\ -\sin(\theta_e) & \cos(\theta_e) \end{bmatrix} \begin{bmatrix} v_d \\ v_q \end{bmatrix} \tag{3.34}$$

When choosing the synchronous frame as a reference, with $\omega_e = \omega_s$, one needs to change ω_b in (3.17) and (3.18) to ω_s.

There are three kinds of fluxes in the induction motors: λ_s – stator flux, λ_m – air gap flux, λ_r – rotor flux. Vector control could be performed with respect to any of these flux space-phasors by attaching the reference system D axis to the respective flux linkage space-phasor direction and by keeping its amplitude under surveillance. A general flux may be defined, with the above cases, as a particular situation [47].

The three flux space-vectors are given by

$$\vec{\lambda_s} = L_s\vec{i_s} + L_m\vec{i_r} \tag{3.35a}$$

$$\vec{\lambda_m} = L_m(\vec{i_s} + \vec{i_r}) \tag{3.35b}$$

$$\vec{\lambda_r} = L_m\vec{i_s} + L_r\vec{i_r} \tag{3.35c}$$

We will introduce the general flux,

$$\vec{\lambda_{ma}} = aL_m(\vec{i_s} + \vec{i_{ra}}) \tag{3.36}$$

Where $\vec{i_{ra}} = \vec{i_r}/a$, $\vec{\lambda_{ra}} = a\vec{\lambda_r}$. Substituting from 3.35a, 3.35b, 3.35c and (3.36 in Equation (3.17) to (3.20), we obtain the following dynamic equations for the induction motor in synchronous frame where the general flux $\vec{\lambda_{ma}}$ is oriented with the D axis:

$$\vec{V_s} = (R_s + (p + j\omega_b)(L_s - aL_m))\vec{i_s}$$

$$+(p + j\omega_b)\vec{\lambda_{ma}} \tag{3.37}$$

$$0 = -(R_r + (p + js\omega_b)(L_r - L_m/a))\vec{i_s}$$

$$+(R_r + (p + js\omega_b)L_r)\frac{\vec{\lambda_{ma}}}{aL_m} \tag{3.38}$$

$$\frac{J}{p_p}\frac{d\omega_r}{dt} = T_e - T_l \tag{3.39}$$

$$T_e = \frac{2}{3}p_p(\lambda_{mad}i_{sq} - \lambda_{maq}i_{sd}) \tag{3.40}$$

$$s = (\omega_b - \omega_r)/\omega_b \tag{3.41}$$

Further we get:

$$s\omega_b = \frac{i_{qa}(1+p\sigma_a\tau_r)}{(\frac{\overrightarrow{\lambda_{ma}}}{aL_m}-\sigma_ai_{da})\tau_r} \tag{3.42}$$

Here $\sigma_a = 1 - \frac{L_m}{aL_r}$ $\tau_r = \frac{L_r}{R_r}$.

$$i_{da}(1 + p\sigma_a\tau_r) = (1 + p\tau_r)\frac{\overrightarrow{\lambda_{ma}}}{aL_m} + s\omega_b\sigma_a\tau_ri_{qa} \tag{3.43}$$

In this thesis, the air-gap flux field oriented vector control is applied. As a consequence, here we choose $a = 1$ to guarantee that the general flux is equal to air gap flux.

$\sigma_a = 1 - \frac{L_m}{L_r}$

$$s\omega_b = \frac{i_{qa}(1+p\sigma_a\tau_r)}{(\frac{\overrightarrow{\lambda_{ma}}}{L_m}-(1-\frac{L_m}{L_r})i_{da})\tau_r} \tag{3.44}$$

Further, during the steady state $p = \frac{d}{dt} = 0$. Because the rotor flux leakage is much smaller than the rotor flux, thus rotor flux is approximately equal to the magnetic flux, that is, $L_m \approx L_r$.

$$s\omega_b = \frac{i_{qa}}{\frac{\overrightarrow{\lambda_{ma}}}{L_m}\tau_r} = \frac{i_{qa}}{i_{da}\tau_r} \tag{3.45}$$

$$T_e = \frac{2}{3}p_pi_{qa}i_{da}L_m = \frac{2}{3}p_pi_{qa}\lambda_m \tag{3.46}$$

$$i_s = i_{da} + j * i_{qa} \tag{3.47}$$

Equations 3.45 through 3.47 will be used for the analysis of instantaneous power control in Chapter 6.

CHAPTER 4

CONTROL METHODS OF THE INDUCTION MOTOR

As a classical control method for induction motors, Direct Torque Control (DTC) is discussed first. To understand the relationship between electromagnetic torque of induction motor and active power, DIPC and DOPC developed in [44] are analyzed.

4.1 Direct Torque Control of Induction Motor

Figure 4.1 shows the drive system with induction motor fed by a three-phase voltage source inverter. Figure 4.2 gives the schematic of DTC. At each switching point, DTC chooses a suitable voltage space vector to control the torque and stator flux within specified bounds. Specifically, the hysteresis controllers compare the estimated electromagnetic torque and stator flux with the desired ones and produce an appropriate error message as a binary number. From a switching table that is based on the relationship between voltage vectors and torque, voltage vectors and stator flux, a corresponding switching state is selected for the voltage source inverter.
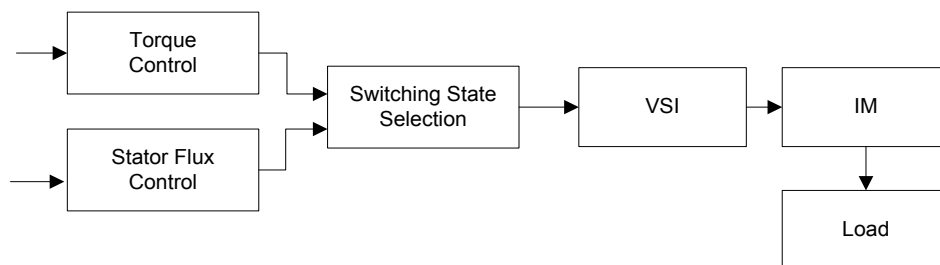
Fig. 4.1 Three-phase voltage source inverter fed induction motor.
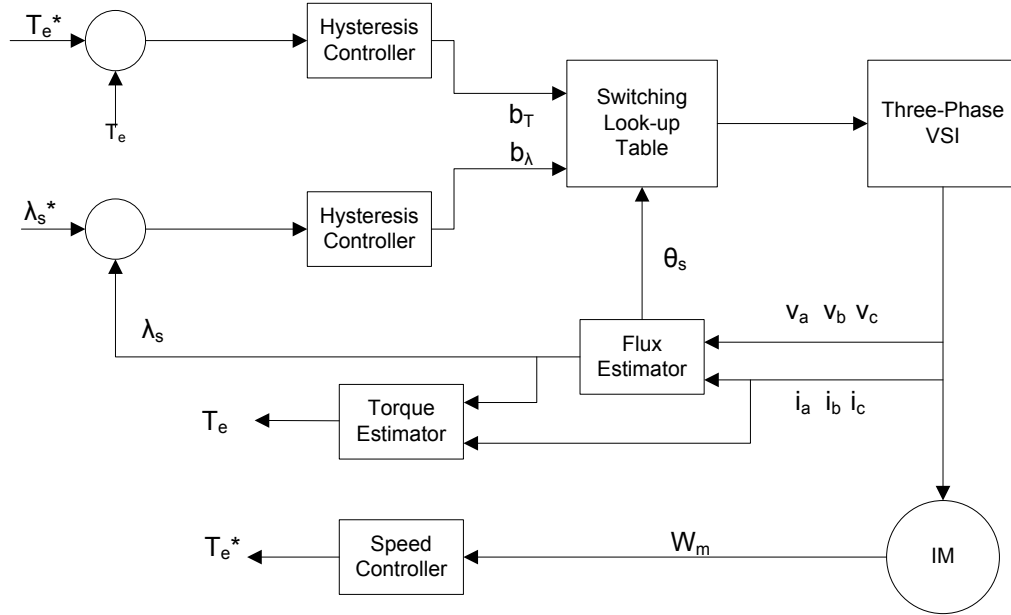
Fig. 4.2 Schematic of direct torque and flux control of induction motor.

4.1.1 Stator Flux of Induction Motor and Voltage Space Vectors

At the stator side, the relationship between stator flux and voltage can be seen from Equation (4.1),

$$\vec{V_s} = R_s \vec{I_s} + \frac{\overrightarrow{d\lambda_s}}{dt} \tag{4.1}$$

If the influence of stator resistance is neglected, the relationship between stator flux and voltage is,

$$\vec{V_s} = \frac{\overrightarrow{d\lambda_s}}{dt} \tag{4.2}$$

We can see that the stator flux always tracks the chosen voltage vector, for example, one electrical cycle later, the stator flux trajectory is a hexagon, as shown in Figure 4.3.
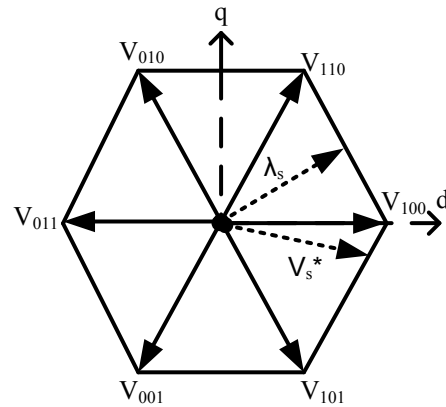
Fig. 4.3 Stator flux trajectory.

Under given operating conditions, each of the non-zero voltage space vectors has a different influence on the magnitude of the stator flux. Generally, we can divide the voltage vectors into two groups: voltage vectors whose relative position to the stator flux vector is less than 90° and that increase the magnitude of stator flux and voltage vector whose relative position to stator flux vector is bigger than 90° and that decrease the magnitude of stator flux. For example, if the stator flux lies in sector I $(-30^\circ, 30^\circ)$, as shown in figure 4.3, the vectors $V_{100}, V_{110}, V_{101}$ will increase the stator flux magnitude, vectors of $V_{010}, V_{011}, V_{001}$ will decrease the stator flux.

4.1.2 Electromagnetic Torque and Voltage Space Vectors

In the field oriented control (FOC), the torque component of stator current is controlled to control the electromagnetic torque. Unlike FOC, the DTC control of the torque of an induction motor is directly based on the relationship between voltage space vectors and torque.

The stator and rotor current vectors are given by,

$$\vec{i_s} = \frac{\vec{\lambda_s} - L_m \vec{i_r}}{L_s} \tag{4.3}$$

$$\vec{i_r} = \frac{\vec{\lambda_r} - L_m \vec{i_s}}{L_r} \tag{4.4}$$

Substituting Equation (4.4) in (4.3), we get,

$$\vec{i_s} = \frac{L_r \vec{\lambda_s} - L_m \vec{\lambda_r}}{L_s L_r - L_m^2} \tag{4.5}$$

Replacing $\vec{i_s}$ in Equation (4.6) with Equation (4.5), we get the following expression for electromagnetic torque,

$$T_e = \frac{2}{3} pp \operatorname{Im}(\vec{i_s} \vec{\lambda_s}^*) \tag{4.6}$$

$$T_e = \frac{2}{3} P_p \operatorname{Im}(\frac{L_r \vec{\lambda_s} - L_m \vec{\lambda_r}}{L_s L_r - L_m^2} \vec{\lambda_s}^*)$$

$$= \frac{2}{3} p_p \frac{L_m}{L_\sigma^2} \operatorname{Im}\left(\vec{\lambda_r} \vec{\lambda_s}^*\right)$$

$$= \frac{2}{3} p_p \frac{L_m}{L_\sigma^2} \operatorname{Im}\left(\vec{\lambda_s} \vec{\lambda_r}^*\right)$$

$$= \frac{2}{3} p_p \frac{L_m}{L_\sigma^2} \lambda_r \lambda_s \sin(\theta_s - \theta_r) \tag{4.7}$$

Here $L_\sigma^2 = L_s L_r - L_m^2$. Equation (4.7) shows that the angle difference between the stator flux and rotor flux will influence the electromagnetic torque. Specifically, the voltage vector leading stator flux will accelerate the rotating speed of stator flux, thus both the angle difference and the torque will increased; while if the voltage vector lags the stator flux, it will accelerate the stator flux in the opposite direction, thus decreasing the angle difference, and reducing the electromagnetic torque. The zero vector leaves the stator flux unchanged.

As long as we know how the stator flux and electromagnetic torque are influenced by voltage vectors, and if the position of the stator flux is known, we can form the following switching look-up table for the voltage source inverter. Here SI represents the flux in the sector I.

Table 4.1. Optimal switching table for DTC of IM

Flux	Torque	SI	SII	SIII	SIV	SV	SVI
	1	110	010	011	001	101	100
1	0	111	000	111	000	111	000
	-1	101	100	110	010	011	001
	1	010	011	001	101	100	110
0	0	000	111	000	111	000	111
	-1	001	101	100	110	010	011

The binary numbers from Table 4.1 come from the flux and torque hysteresis controller shown in Figures 4.4 and 4.5. We define the following rules for the torque and flux hysteresis controller.
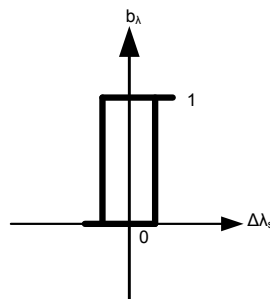

Fig. 4.4 Flux hysteresis controller.
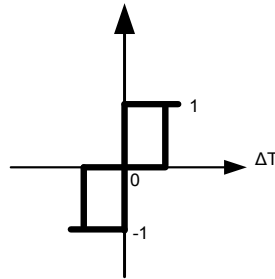
Fig. 4.5 Torque hysteresis controller.

For the stator flux controller, $\Delta\lambda_s = \lambda_s^* - \lambda_s$.

If $\Delta\lambda_s > \lambda_{th}$; or $-\lambda_{th} < \Delta\lambda_s < \lambda_{th}$ and $\frac{d\Delta T}{dt} < 0$, b_λ = 1, then λ_s must be increased. Otherwise b_λ = 0 and λ_s needs must be decreased.

For the torque controller, we use three level controls, $\Delta T = T_e^* - T_e$.

$\Delta T \geq T_{th}$; or $\Delta T > 0$ and $\frac{d\Delta T}{dt} < 0$, $b_T = 1$

$\Delta T \leq -T_{th}$; or $\Delta T < 0$ and $\frac{d\Delta T}{dt} > 0$, $b_T = -1$

Otherwise; $b_T = 0$

Here, λ_{th} and T_{th} are the hysteresis controller bands for the stator flux and electromagnetic torque, respectively.

4.1.3 Stator Flux Sector Definition

The variable S is the number of the sector where the stator flux lies. There are 6 sectors as shown in Figure 4.3 and the sectors are defined in Equation (4.8). The value of S for b_λ = (0,1) and b_T= (-1, 0, 1) is given by:

$$S = 3b_\lambda + b_T + 2 \tag{4.8}$$

The torque equation is given as (4.9),

$$T_e = \frac{2}{3} p_P \left(\lambda_{sd} i_{sq} - \lambda_{sq} i_{sd} \right) \tag{4.9}$$

The stator flux is,

$$\lambda_s = \int_0^t \overrightarrow{u_s} - R_s \overrightarrow{i_s} \tag{4.10}$$

As for the reference torque, it is obtained from the speed PI controller that uses the reference mechanical speed and actual mechanical speed as its inputs.

The simulation results with DTC are compared with those of DIPC and DOPC in Section 4.3 and 4.4.

4.2 Power Flow Within Induction Motor

The literature on electric machinery includes many discussions of the issue of power within the induction motor. From the viewpoint of energy conversion, the induction motor converts electrical energy to mechanical energy. In the following chapter, the active power distribution in the steady state is analyzed for the DIFC and DOFC methods.

Various losses account for the difference between input active power and output mechanical power. At the stator side, the losses include the stator winding loss and core loss, as given by

$$P_{loss} = P_{loss\_s} + P_{loss\_core} \tag{4.11}$$

Subtracting the stator losses from the input power, we can get the electromagnetic power - P_e that can be decoupled into four different parts,

$$P_e = P_{loss\_r} + P_{loss\_m} + P_{loss\_other} + P_m \qquad (4.12)$$

where, P_{loss_r} is the rotor winding loss, P_{loss_m} is the mechanical loss, and P_m is the mechanical output power, P_{loss_other} is the other losses. The total active power balance is

$$P_{in} = P_s + P_e \qquad (4.13)$$

In an idealized induction motor, we usually ignore various losses except for the power consumed by the rotor resistance. The input real power is then expressed as the sum of the mechanical power and the power consumed by resistance, i.e.

$$P_{in} = P_{loss\_s} + P_m \qquad (4.14)$$

$$P_m = T_e w_m \qquad (4.15)$$

From equation (4.15), the mechanical power is proportional to the electromagnetic torque in the steady state. This inspires us to apply the control principle of torque to the control of output power.

Substituting for P_m in equation (4.14) from (4.15), we get

$$P_{in} = P_{loss\_s} + T_e w_m \qquad (4.16)$$

Based on such a relationship, the input real power control of induction motor is found. It can be employed in a control technique that realizes the torque control as well.

4.3 Principles of the DIPC and DOPC

The main reason that we want to replace the electromagnetic torque with active power in the control scheme is that the electromagnetic torque is difficult to be measured. In contrast to the torque, the active power can be easily calculated from the monitored current and voltage. In addition, the power control is expected to provide better dynamic performance, as it essentially involves stator voltage and current. The author of reference [44] proposes two new methods for the control of an induction motor. They are direct output power and flux control versus direct input power and flux control. The control of stator flux in both methods is the same as in DTC. Regarding the output control,

$$P_m = P_{out} = \frac{2}{3} \frac{L_m}{L_\sigma^2} w_r \lambda_s \lambda_r \sin(\theta_s - \theta_r) \qquad (4.17)$$

The output power is influenced by the angle difference between stator and rotor flux. Such a relationship indicates that the working principle of DTC can also be applied to the direct output power and flux control. The reference output power is given by

$$P_{out} = T_e{}^* w_m{}^* \qquad (4.18)$$

and the estimated output power can be obtained from Equation (4.15). Figure 4.6 shows the schematic of this control approach.
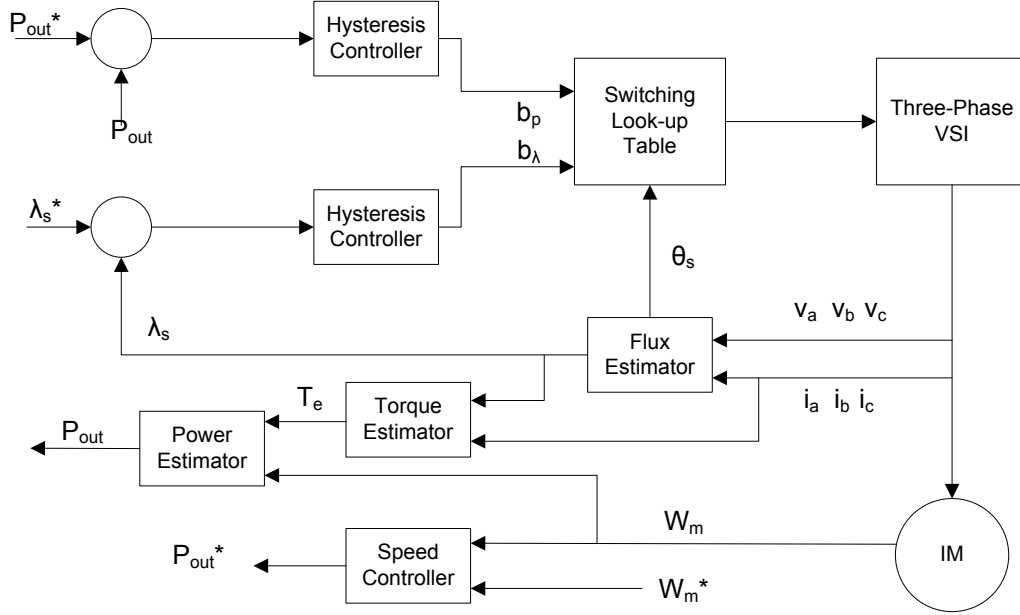
Fig. 4.6 Schematic of direct output power and flux control.

Unlike the output power, the input power is not only dependent on stator and rotor angle difference, but is also influenced by the slip frequency as follows

$$P_{in} = \frac{2}{3}\frac{L_m}{L_\sigma^2 r}(w_r + w_{sl})\lambda_s\lambda_r\sin(\theta_s - \theta_r)$$

$$= \frac{2}{3}\frac{L_m}{L_\sigma^2 r}(w_r)\lambda_s\lambda_r\sin(\theta_s - \theta_r)$$

$$+ \frac{2}{3}\frac{L_m}{L_\sigma^2 r}(w_{sl})\lambda_s\lambda_r\sin(\theta_s - \theta_r) \tag{4.19}$$

Comparing Equation (4.19) with Equation (4.17), the former can be taken as the sum of the output power and the power related to slip-speed. In the reference input power, we must compensate for the slip-speed part. Reference [44] adopts the following compensation technique:

$$P_{in}{}^* = T_e(w_m{}^* + w_{sl}{}^*) \tag{4.20}$$

$$w_{sl}{}^* = k_{sl}(w_m{}^* - w_m) \tag{4.21}$$

The estimation of input power can be obtained from Equation (4.22)

$$P_{in} = T_e w_s = T_e(w_r + w_{sl})/P_p \tag{4.22}$$
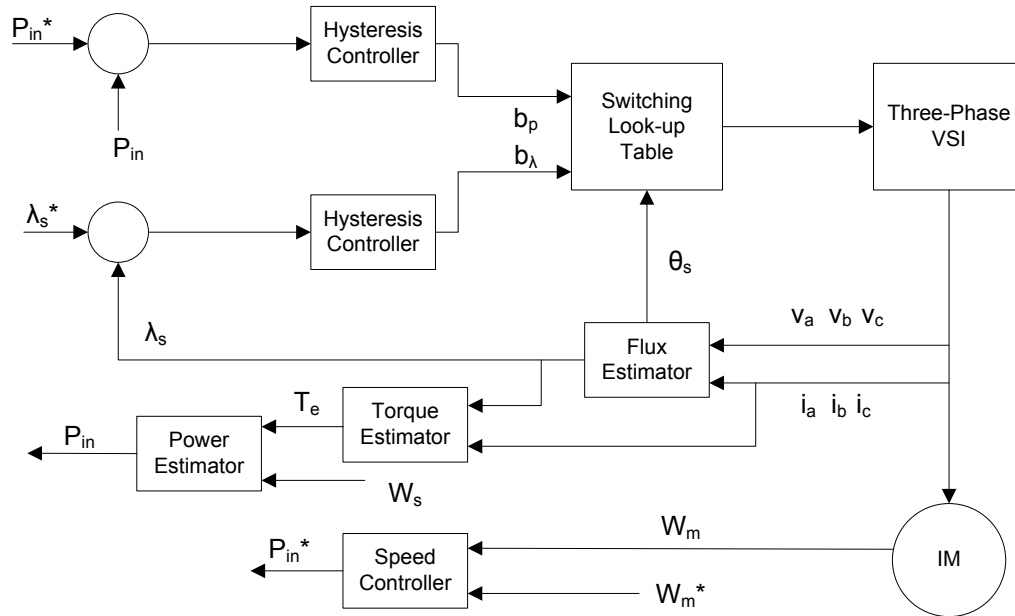
Fig. 4.7 Schematic of direct input power and flux control of induction motor.

We can use the same for the direct input power and flux control. The general schematic of direct input power and flux control is given in Figure 4.7.

4.4 Simulation Results for DTC, DIPC and DOPC.

The induction motor in APPENDIX has been used in the simulations. The input DC voltage for the three-phase voltage source inverter is 330 volts. The switching frequency is 50 kHz; the reference stator flux is $0.7\ W$b, The hysteresis band for the stator flux is $0.005\ Wb$. The reference speed ramps up to 110 rad/sec at 0.6 seconds and then remains constant. The load torque jumps from zero to $60\ \mathrm{N.m}$ at 1.0 s, and jumps again,

to $30\,\text{N.m}$ at 1.5 s. The electromagnetic torque and speed profile resulting from the three methods described in the preceding section are shown in Figures 4.8 to 4.13.
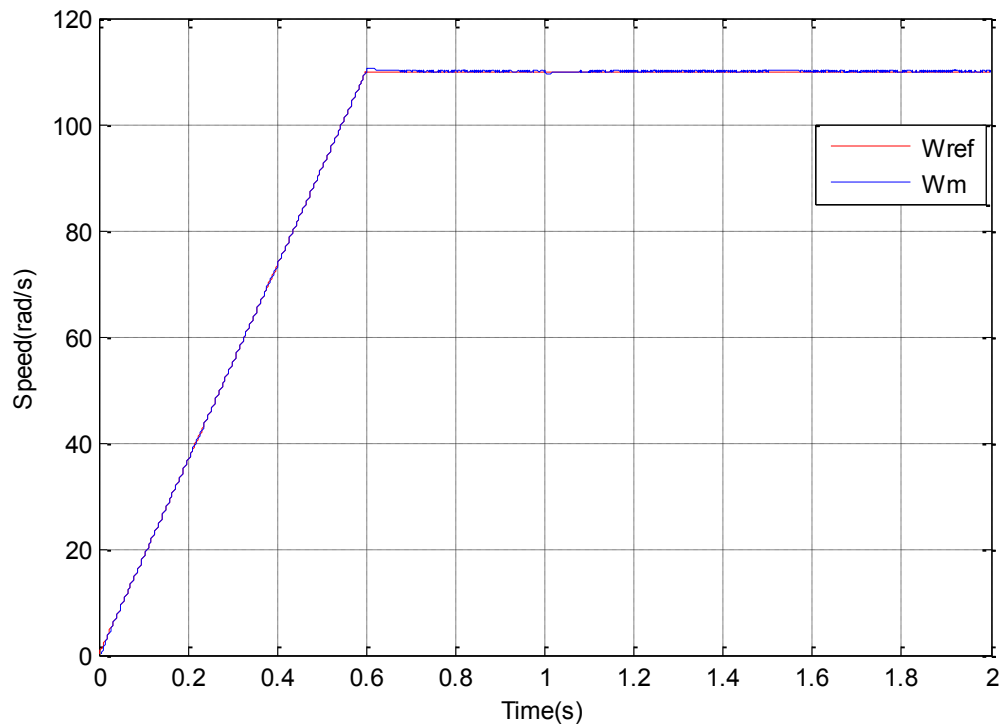
Fig. 4.8 Reference and estimated mechanical speeds at DTC.
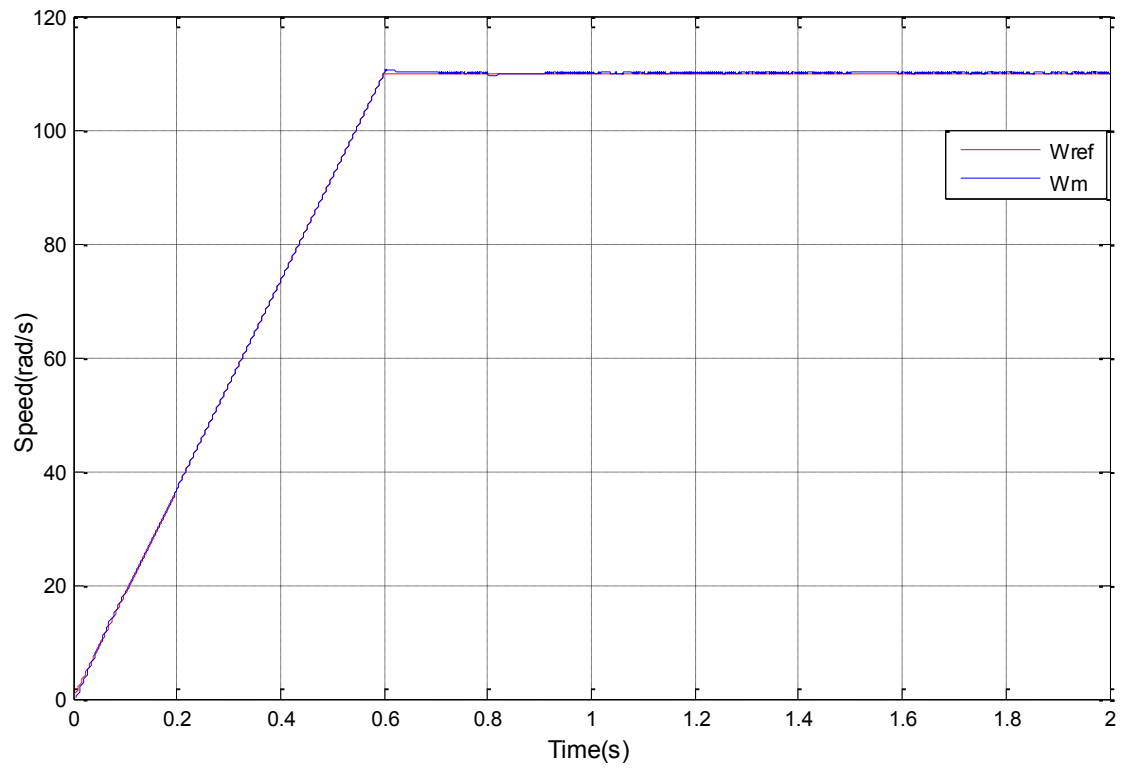
Fig. 4.9 Reference and estimated mechanical speeds at DOPC.
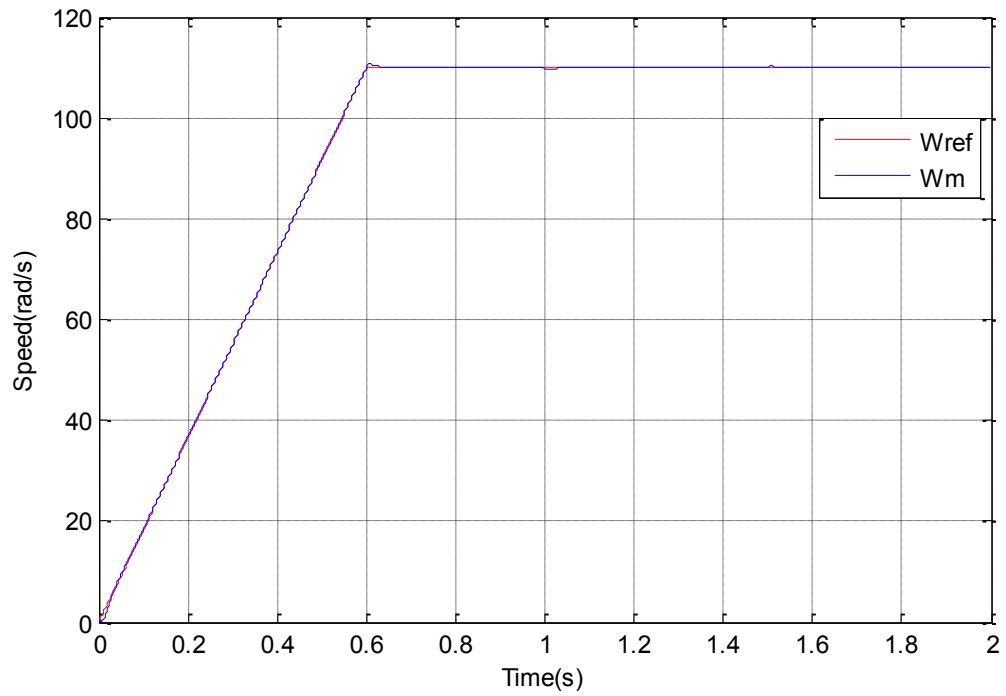
Fig. 4.10 Reference and estimated mechanical speeds at DIPC.
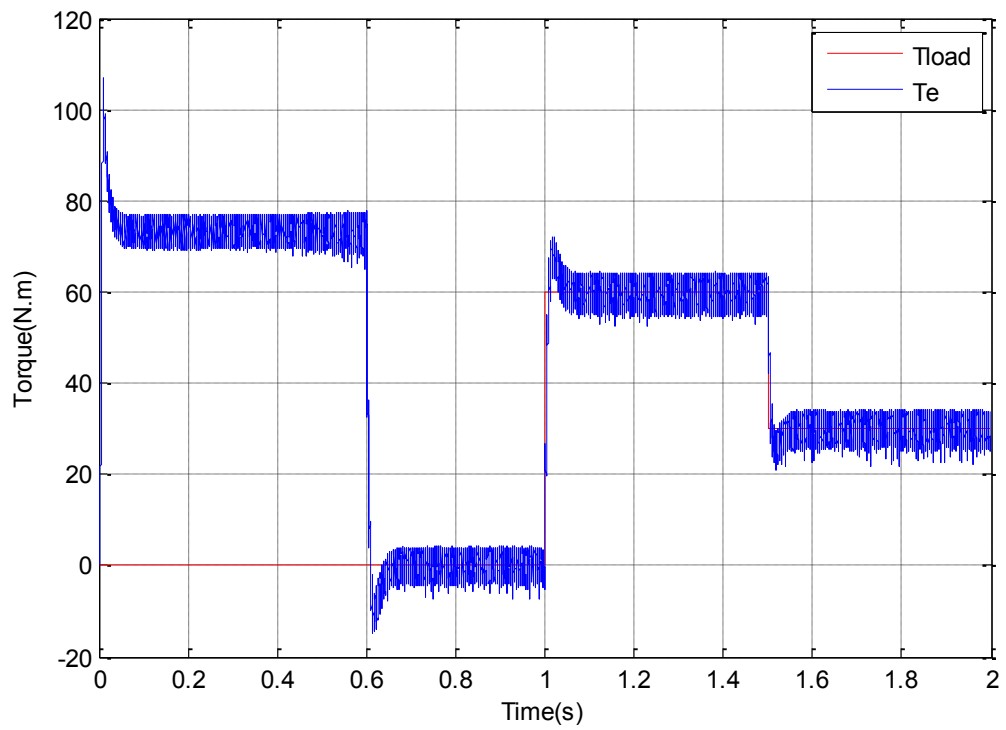
Fig. 4.11 Load torque and electromagnetic torque at DTC.
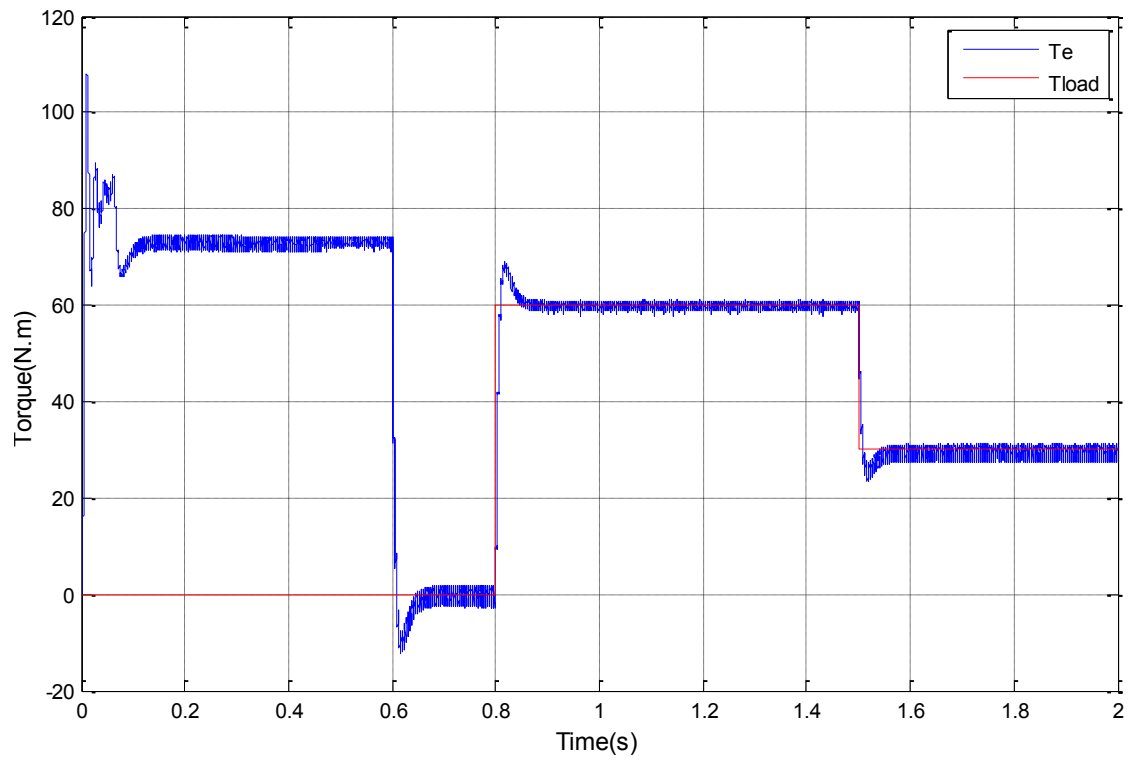
Fig. 4.12 Load torque and electromagnetic torque at DOPC.
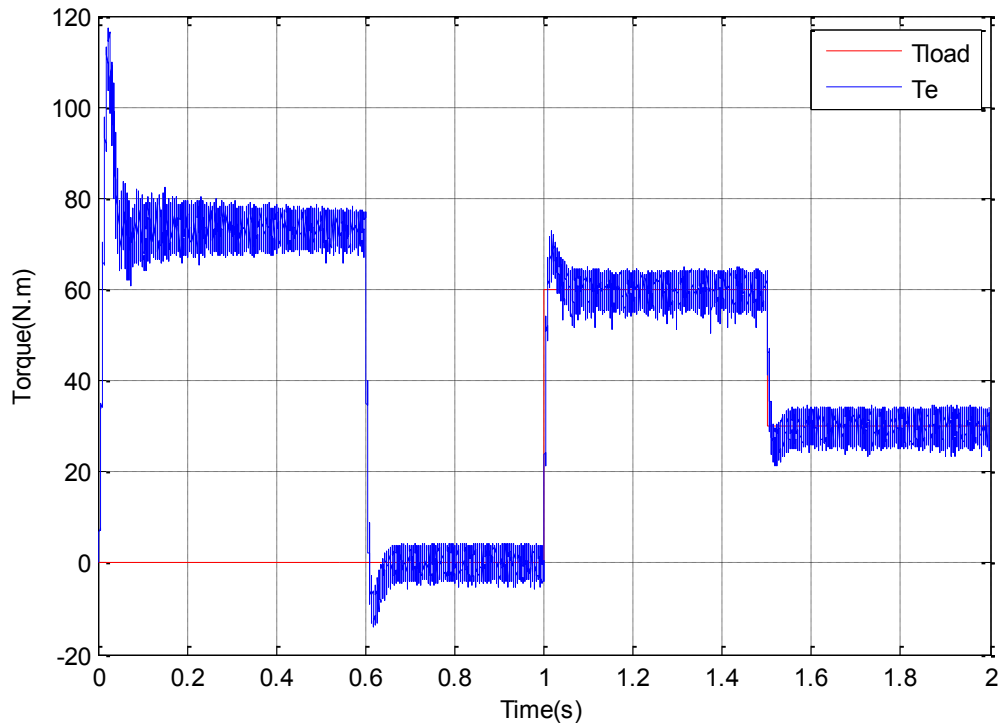
Fig. 4.13 Load torque and electromagnetic torque at DIPC.

It can be concluded that power control provides similar electromagnetic torque and speed trajectories as does torque control.

4.5 Conclusion

DTC, DIPC and DOPC utilize the voltage space vector's impact on electromagnetic torque, input power, and output power as well as its affect on stator flux to drive the torque, power, and flux to their desired levels, they are essentially the same.

CHAPTER 5

INSTANTANEOUS ELECTRIC POWERS

The dynamics and energy flow of induction motors have been researched since 1920s. The theories dealing with the instantaneous active power and reactive power can be classified into two kinds: *p-q* theory and *abc* theory [48]. In this chapter the emphasis is on *p-q* theory. In power electronics, the concept of instantaneous power has been used in control of PWM rectifiers. In electric drive systems, Betz et al. used the idea of instantaneous powers to control induction motor drives. Lee et al. adapted this idea to improve the performance of induction motor fed by matrix converter. Control methods in [31-40] are based on the idea that active power is related to torque and reactive power is related to flux in the synchronous reference frame. As for the relationship between torque and stator flux and the instantaneous active and reactive power in the stationary reference frame, no relevant literatures have been found by this researcher. In this chapter, observations regarding the relationship between the instantaneous powers and the torque and flux of induction motor in the stationary reference frame are given with the support of simulations.

5.1 P-Q Theory

Akagi was the first to propose the *p-q* theory in [48]. The *p-q* theory utilizes the Clark transformation described in Chapter 3 to express the instantaneous active and reactive power that as.

$$p = \frac{2}{3}\left(v_d i_d + v_q i_q\right) \qquad\qquad (5.1)$$

$$q = \frac{2}{3}\left(v_q i_d - v_d i_q\right) \tag{5.2}$$

where v_d and v_q are the d-q components of the stator voltage vector and i_d and i_q are the d-q components of the stator current vector.

P-q theory provides specific physical meanings to instantaneous powers. For the instantaneous active power, the definition is as follows:

"For a three-phase system with or without a neutral conductor in the steady state or during transients, the three-phase instantaneous active power p describes the total instantaneous energy flow per second between two subsystems."

For the instantaneous reactive power, its definition is given as,

"The imaginary power q is proportional to the quantity of energy that is being exchanged between the phases of the system. It does not contribute to the energy transfer between the source and the load at any time."

The physical meaning of active power is easy to understand, while the explanation of reactive power is somewhat abstract. In the three-phase induction motor, reactive power represents the energy exchanged among the A, B, and C phase per second. However, it is difficult to determine how much reactive power the voltage source inverter should provide at each switching cycle to keep the motor working as required.

5.2 Input Active and Reactive Power Versus Voltage Space Vectors

As mentioned in Chapter 3, there are 8 switching states in the three-phase voltage source inverter. Consequently, for the induction motor fed by this kind of inverter, there

are eight input active and reactive power pairs. The analysis of these powers is incritical in this research. With the help of Equations (3.13), (5.1) and (5.2), we get the following table:

Table 5.1. Input active and reactive powers

Voltage Space Vector	Input Active Power	Input Reactive Power
V_{100}	$\frac{1}{3}v_i(2i_{s,d})$	$-\frac{1}{3}v_i(2i_{s,q})$
V_{110}	$\frac{1}{3}v_i(i_{s,d}+\sqrt{3}i_{s,q})$	$\frac{1}{3}v_i(\sqrt{3}i_{s,d}-i_{s,q})$
V_{010}	$\frac{1}{3}v_i(\sqrt{3}i_{s,q}-i_{s,d})$	$\frac{1}{3}v_i(\sqrt{3}i_{s,d}+i_{s,q})$
V_{011}	$-\frac{1}{3}v_i(2i_{s,d})$	$\frac{1}{3}v_i(2i_{s,q})$
V_{001}	$-\frac{1}{3}v_i(i_{s,d}+\sqrt{3}i_{s,q})$	$-\frac{1}{3}v_i(\sqrt{3}i_{s,d}-i_{s,q})$
V_{101}	$-\frac{1}{3}v_i(\sqrt{3}i_{s,q}-i_{s,d})$	$-\frac{1}{3}v_i(\sqrt{3}i_{s,d}+i_{s,q})$
$V_{000/111}$	0	0

Here $i_{s,d}$, $i_{s,q}$ are the d and q components of the stator current vector, respectively, and v_i is the input voltage of the inverter. The voltage space vectors V_{011}, V_{001} and V_{101} have input active and reactive power of different polarity than those of V_{100}, V_{110}, and V_{010}. Note that the powers for zero vectors are zeros.

For the active and reactive power, their sign depends on the relative position of the voltage and current waveforms. Specifically, the definition of the active and reactive power are.
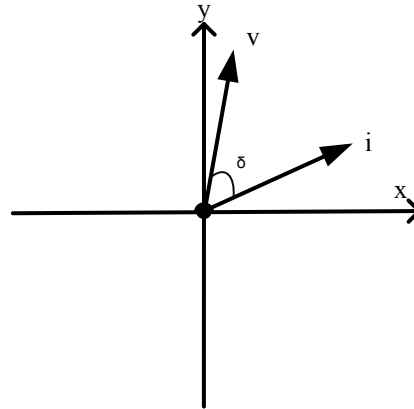
Fig. 5.1 Phasor diagram of voltage and current.

$$Q = v\,i\sin(\delta) \tag{5.3}$$

$$P = v\,i\cos(\delta) \tag{5.4}$$

where δ is the angle difference between voltage and current waveforms, as illustrated in Figure 5.3. As for the instantaneous powers, as long as the position of stator current vector is known, we can determine the sign of reactive and active power for each voltage space vector based on Equations (5.3) and (5.4).

If the load is inductive, the consumed reactive power is positive; if the load is capacitive, it is negative. The induction motor can be considered as an inductive load. Therefore, at each switching period, the voltage vectors that will produce positive reactive power will be considered to be selected to control the motor.

Typically the active power is positive, if the power goes from the source to the load, and negative, if the power goes from the load to source. The induction machine in this research always operates as a motor, and the active power it needs is always positive. In other words, voltage space vectors that produce positive active power will be considered to control the motor.

5.3 Analysis of Instantaneous Powers

The induction motor can be represented by an assembly of inductances, resistances and a voltage source at the rotor side. We can regard it as an inductive load with a three-phase balanced voltage source. If we know how the torque and flux changes under given active and reactive power, we can control the input powers to control the torque and flux. The steady state relationship between torque and input active power is given In Chapter 4. Here, we first discuss the power distribution within the induction motor then provide general formulas for the transient state.

5.3.1 Instantaneous Power Distribution

Induction motor converts the electrical power to mechanical power to drive loads. Specifically, the mechanical power at the rotor side is expressed as,

$$P_{mech} = T_e \frac{w_r}{p_p} \tag{5.5}$$

while the rest of active power is consumed by the resistances and the inductances, For a resistance, the instantaneous apparent power $\vec{s}_R$, is given by

$$\vec{s}_R = \vec{v}_R \vec{i}_R^* / 1.5 = R \vec{i}_R \vec{i}_R^* / 1.5 = R i_R^2 / 1.5 \tag{5.6}$$

so,

$$p_R = Ri_R^2/1.5 = R(i_{R,d}^2 + i_{R,q}^2)/1.5 \qquad (5.7)$$

and,

$$q_R = 0 \qquad (5.8)$$

Considering the stator and rotor resistance, the total instantaneous active power consumed is,

$$P_R = \frac{2}{3}R_r\left(i_{r,d}^2 + i_{r,q}^2\right) + \frac{2}{3}R_s\left(i_{s,d}^2 + i_{s,q}^2\right) \qquad (5.9)$$

Regarding the inductance L, the apparent power consumed is,

$$\vec{s}_L = \vec{v}_L \vec{i}_L^*/1.5$$

$$= L\frac{d\vec{i}_L}{dt}\vec{i}_L^*/1.5$$

$$= \frac{2}{3}L\left(\frac{di_{L,d}}{dt} + j\frac{di_{L,q}}{dt}\right)(i_{L,d} - ji_{L,q})$$

$$= \frac{2}{3}L\left(i_{L,d}\frac{di_{L,d}}{dt} + i_{L,q}\frac{di_{L,q}}{dt}\right) + j\frac{2}{3}L\left(i_{L,d}\frac{di_{L,q}}{dt} - i_{L,q}\frac{di_{L,d}}{dt}\right) \quad (5.10)$$

Thus,

$$p_L = L\left(i_{L,d}\frac{di_{L,d}}{dt} + i_{L,q}\frac{di_{L,q}}{dt}\right)/1.5 \qquad (5.11)$$

and

$$q_L = L\left(i_{L,d}\frac{di_{L,q}}{dt} - i_{L,q}\frac{di_{L,d}}{dt}\right)/1.5 \qquad (5.12)$$

From Equation (5.11), we find that the instantaneous active power for the inductance in transient states is not zero, as power is delivered to it and retrieved from it. The inductance in the induction motor are the stator leakage inductance, the rotor leakage inductance, and the magnetizing inductance. So the total instantaneous active power for all these inductances is,

$$P_L = \frac{2}{3}L_{lr}\left(i_{r,d}\frac{di_{r,d}}{dt} + i_{r,q}\frac{di_{r,q}}{dt}\right) + \frac{2}{3}L_{ls}\left(i_{s,d}\frac{di_{s,d}}{dt} + i_{s,q}\frac{di_{s,q}}{dt}\right)$$

$$+ \frac{2}{3}L_m\left((i_{s,d}+i_{r,d})\frac{d(i_{s,d}+i_{r,d})}{dt} + (i_{s,q}+i_{r,q})\frac{d(i_{s,q}+i_{r,q})}{dt}\right)\ (5.13)$$

The instantaneous reactive power is only in the inductances and is given by

$$Q_L = \frac{2}{3}L_{ls}\left(i_{s,d}\frac{di_{s,q}}{dt} - i_{s,q}\frac{di_{s,d}}{dt}\right) + \frac{2}{3}L_{lr}\left(i_{r,d}\frac{di_{r,q}}{dt} - i_{r,q}\frac{di_{r,d}}{dt}\right)$$

$$+ \frac{2}{3}L_m\left((i_{s,d}+i_{r,d})\frac{d(i_{s,q}+i_{r,q})}{dt} - (i_{s,q}+i_{r,q})\frac{d(i_{s,d}+i_{r,d})}{dt}\right)(5.14)$$

Rearranging Equations (5.13) and (5.14) to express power with a combination of current and flux rather than only current, yields,

$$P_L = \frac{2}{3}\left(i_{s,d}\frac{d\lambda_{s,d}}{dt} + i_{s,q}\frac{d\lambda_{s,q}}{dt}\right) + \frac{2}{3}\left(i_{r,d}\frac{d\lambda_{r,d}}{dt} + i_{r,q}\frac{d\lambda_{r,q}}{dt}\right) \qquad (5.15)$$

$$Q_L = \frac{2}{3}\left(i_{s,d}\frac{d\lambda_{s,q}}{dt} - i_{s,q}\frac{d\lambda_{s,d}}{dt}\right) + \frac{2}{3}\left(i_{r,d}\frac{d\lambda_{r,q}}{dt} - i_{r,q}\frac{d\lambda_{r,d}}{dt}\right) \qquad (5.16)$$

The sum of Equations (5.5), (5.9) and (5.15) is the total instantaneous active power, that is,

$$P_{total} = P_L + P_R + P_{mech}$$

$$= \frac{2}{3}\left(i_{s,d}\frac{d\lambda_{s,d}}{dt} + i_{s,q}\frac{d\lambda_{s,q}}{dt}\right) + \frac{2}{3}\left(i_{r,d}\frac{d\lambda_{r,d}}{dt} + i_{r,q}\frac{d\lambda_{r,q}}{dt}\right)$$

$$+ \frac{2}{3}R_s\left(i_{s,d}^2 + i_{s,q}^2\right) + \frac{2}{3}R_r\left(i_{r,d}^2 + i_{r,q}^2\right) + \frac{T_e\omega_r}{P_p} \qquad (5.17)$$

Since the reactive power is only in the inductances, Equation (5.16) gives the total instantaneous reactive power, that is,

$$Q_{total} = \frac{2}{3}\left(i_{s,d}\frac{d\lambda_{s,q}}{dt} - i_{s,q}\frac{d\lambda_{s,d}}{dt}\right) + \frac{2}{3}\left(i_{r,d}\frac{d\lambda_{r,q}}{dt} - i_{r,q}\frac{d\lambda_{r,d}}{dt}\right) \qquad (5.18)$$

From Equation (5.17) it can be seen that the expression for the total active power contains the electromagnetic torque. Equation (5.19) demonstrates the relationship between active power and the angle difference [44],

$$P_{total} = P_{in} = \frac{2}{3}\frac{L_m}{L_\sigma^2}\omega_s|\lambda_s||\lambda_r|\sin(\theta_s - \theta_r) \qquad (5.19)$$

where $L_\sigma^2 = L_sL_r - L_m^2$. Thus, input power and torque can be controlled by adjusting the angle difference between stator flux and rotor flux.

To relate stator flux and reactive power, we use the following expressions for the currents $i_{s,d}$, $i_{s,q}$, $i_{r,d}$, and $i_{r,q}$.

$$i_{s,d} = \frac{L_r\lambda_{s,d} - L_m\lambda_{r,d}}{L_\sigma^2} \qquad (5.20)$$

$$i_{s,q} = \frac{L_r\lambda_{s,q} - L_m\lambda_{r,q}}{L_\sigma^2} \qquad (5.21)$$

$$i_{r,d} = \frac{L_s\lambda_{r,d} - L_m\lambda_{s,d}}{L_\sigma^2} \qquad (5.22)$$

$$i_{r,q} = \frac{L_s\lambda_{r,q} - L_m\lambda_{s,q}}{L_\sigma^2} \qquad (5.23)$$

Then we substitute in (5.18) to obtain

$$Q_{total} = \frac{2}{3}\frac{L_r}{L_\sigma^2}\lambda_s{}^2 \frac{\left(\lambda_{s,d}\frac{d\lambda_{s,q}}{dt}-\lambda_{s,q}\frac{d\lambda_{s,d}}{dt}\right)}{\lambda_{s,d}{}^2+\lambda_{s,q}{}^2} + \frac{2}{3}\frac{L_s}{L_\sigma^2}\lambda_r{}^2 \frac{\left(\lambda_{r,d}\frac{d\lambda_{r,q}}{dt}-\lambda_{r,q}\frac{d\lambda_{r,d}}{dt}\right)}{\lambda_{r,d}{}^2+\lambda_{r,q}{}^2}$$

$$-\frac{2}{3}\frac{L_m}{L_\sigma^2}\lambda_{r,d}{}^2 \frac{\left(\lambda_{r,d}\frac{d\lambda_{s,q}}{dt}-\lambda_{s,q}\frac{d\lambda_{r,d}}{dt}\right)}{\lambda_{r,d}{}^2} - \frac{2}{3}\frac{L_m}{L_\sigma^2}\lambda_{s,d}{}^2 \frac{\left(\lambda_{s,d}\frac{d\lambda_{r,q}}{dt}-\lambda_{r,q}\frac{d\lambda_{s,d}}{dt}\right)}{\lambda_{s,d}{}^2}$$

$$(5.24)$$

We also need the identities

$$\omega_s = \frac{\left(\lambda_{s,d}\frac{d\lambda_{s,q}}{dt}-\lambda_{s,q}\frac{d\lambda_{s,d}}{dt}\right)}{\lambda_{s,d}{}^2+\lambda_{s,q}{}^2} \qquad (5.25)$$

$$\omega_s = \frac{\left(\lambda_{r,d}\frac{d\lambda_{r,q}}{dt}-\lambda_{r,q}\frac{d\lambda_{r,d}}{dt}\right)}{\lambda_{r,d}{}^2+\lambda_{r,q}{}^2} \qquad (5.26)$$

$$\frac{d}{dt}\left(\frac{\lambda_{s,q}}{\lambda_{r,d}}\right) = \frac{\left(\lambda_{r,d}\frac{d\lambda_{s,q}}{dt}-\lambda_{s,q}\frac{d\lambda_{r,d}}{dt}\right)}{\lambda_{r,d}{}^2} \qquad (5.27)$$

$$\frac{d}{dt}\left(\frac{\lambda_{r,q}}{\lambda_{s,d}}\right) = \frac{\left(\lambda_{s,d}\frac{d\lambda_{r,q}}{dt}-\lambda_{r,q}\frac{d\lambda_{s,d}}{dt}\right)}{\lambda_{s,d}{}^2} \qquad (5.28)$$

Thus, the instantaneous reactive power can be expressed as,

$$Q_{total} = \frac{2}{3}\frac{L_r}{L_\sigma^2}\lambda_s{}^2\omega_s + \frac{2}{3}\frac{L_s}{L_\sigma^2}\lambda_r{}^2\omega_s - \frac{2}{3}\frac{L_m}{L_\sigma^2}\lambda_{r,d}{}^2\frac{d}{dt}\left(\frac{\lambda_{s,q}}{\lambda_{r,d}}\right)$$

$$-\frac{2}{3}\frac{L_m}{L_\sigma^2}\lambda_{s,d}{}^2\frac{d}{dt}\left(\frac{\lambda_{r,q}}{\lambda_{s,d}}\right) \qquad (5.29)$$

From Equation (5.28), we can find that during transient states, the instantaneous reactive power is related to the square of stator flux and rotor flux, and the interaction

between stator and rotor flux. In the steady state, the change in the total instantaneous reactive power will influence the change of stator flux. The derivative of both sides of Equation (5.29) gives,

$$\frac{dQ_{total}}{dt} = \frac{2}{3}\frac{L_r}{L_\sigma^2}\lambda_s \cdot \frac{d\lambda_s}{dt}\omega_s - \frac{2}{3}\frac{d}{dt}\left(\frac{L_m}{L_\sigma^2}\lambda_{r,d}^2\frac{d}{dt}\left(\frac{\lambda_{s,q}}{\lambda_{r,d}}\right)\right)$$

$$- \frac{2}{3}\frac{d}{dt}\left(\frac{L_m}{L_\sigma^2}\lambda_{s,d}^2\frac{d}{dt}\left(\frac{\lambda_{r,q}}{\lambda_{s,d}}\right)\right) \tag{5.30}$$

It can be seen that the change in the total reactive power is related to the second and third terms in Equation (5.30). If these two terms are sufficiently small, we could conclude that the increase in total reactive power will cause an increase in stator flux and vice versa.

Alternatively, with the help of equations,

$$\lambda_{s,d} = |\lambda_s|\cos(\theta_s) \tag{5.31}$$

$$\lambda_{s,q} = |\lambda_s|\sin(\theta_s) \tag{5.32}$$

$$\lambda_{r,d} = |\lambda_r|\cos(\theta_r) \tag{5.33}$$

$$\lambda_{r,q} = |\lambda_r|\sin(\theta_r) \tag{5.34}$$

we can rewrite Equation (5.24) as,

$$Q_{total} = \frac{2}{3}\frac{L_r}{L_\sigma^2}\lambda_s^2\omega_s + \frac{2}{3}\frac{L_s}{L_\sigma^2}\lambda_r^2\omega_s - \frac{4}{3}\frac{L_m}{L_\sigma^2}\omega_s|\lambda_s||\lambda_r|\cos(\theta_s - \theta_r)$$

$$\tag{5.35}$$

From Equation (5.35), it can be seen that the instantaneous reactive power is not only related to the stator flux, but also to the angle difference between stator flux and rotor flux. Note that the active power is also related to this angle difference. Therefore, we can conclude that the stator flux is related to both the active and reactive power.

5.3.2 Simplified Approach to the P-Q Analysis

In 5.3.1, an accurate analysis of active and reactive power distribution and their relationship with torque and flux were attempted. Since at each switching period, the choice of voltage space vector for three-phase inverter is limited, a simplified power analysis is acceptable.

The related assumptions are:

(1) The leakage inductances are negligible in comparison with the magnetizing inductance L_m. Consequently, the whole reactive power is consumed by L_m.

(2) The voltage drop across the stator resistance and leakage reactance is negligible in comparison with the stator voltage V_s. Thus the voltage across L_m equals V_s.

The powers consumed by Lm are given by

$$p_m = \frac{2}{3}\left(i_{m,d}\frac{d\lambda_{m,d}}{dt} + i_{m,q}\frac{d\lambda_{m,q}}{dt}\right) \tag{5.36}$$

$$q_m = \frac{2}{3}\left(i_{m,d}\frac{d\lambda_{m,q}}{dt} - i_{m,q}\frac{d\lambda_{m,d}}{dt}\right) \tag{5.37}$$

As

$$i_{m,d} = \frac{\lambda_{m,d}}{L_m} \tag{5.38}$$

$$i_{m,q} = \frac{\lambda_{m,q}}{L_m} \tag{5.39}$$

$$\frac{d\lambda_{m,d}}{dt} = v_{s,d} \tag{5.40}$$

$$\frac{d\lambda_{m,q}}{dt} = v_{s,q} \tag{5.41}$$

then

$$p_m = \frac{2}{3L_m}(v_{s,d}\lambda_{m,d} + v_{s,q}\lambda_{m,q}) \tag{5.42}$$

$$q_m = \frac{2}{3L_m}(v_{s,q}\lambda_{m,d} - v_{s,d}\lambda_{m,q}) \tag{5.43}$$

Solving these equations for $\lambda_{m,d}$ and $\lambda_{m,q}$ yields

$$\lambda_{m,d} = 1.5\frac{L_m}{v_s^2}(p_m v_{s,d} + q_m v_{s,q}) \tag{5.44}$$

$$\lambda_{m,q} = 1.5\frac{L_m}{v_s^2}(p_m v_{s,q} - q_m v_{s,d}) \tag{5.45}$$

Squaring (5.44) and (5.45) to power 2 and adding gives

$$\lambda_m = 1.5\frac{L_m}{v_s}\sqrt{p_m^2 + q_m^2} \tag{5.46}$$

The real power input to the motor equals

$$p_{in} = \frac{2}{3}(v_{s,d}i_{s,d} + v_{s,q}i_{s,q}) \tag{5.47}$$

and it contains three components: (1) mechanical output power p_{out}, (2) power lost in resistances, p_R, and (3) power delivered to (and recovered from) the magnetizing inductance, p_m. These are given by:

$$p_{out} = T_M \omega_M \tag{5.48}$$

$$p_R = \frac{2}{3}(R_s i_s^2 + R_r i_r^2) \tag{5.49}$$

$$p_m = \frac{2}{3}\left[(i_{s,d} + i_{r,d})v_{s,d} + (i_{s,q} + i_{r,q})v_{s,q}\right] \tag{5.50}$$

From Equations (5.48)-(5.50) it follows that

$$T_M = \frac{1}{\omega_M}(p_{in} - p_R - p_m) \tag{5.51}$$

which clearly shows a direct relation between the torque and real power. On the other hand, substituting

$$p_m = \frac{2}{3}(i_{m,d}v_{s,d} + i_{m,q}v_{s,q}) \tag{5.52}$$

$$q_m = \frac{2}{3}(i_{m,d}v_{s,q} - i_{m,q}v_{s,d}) \tag{5.53}$$

In Equation (5.46) yields,

$$s_m = \sqrt{p_m^2 + q_m^2} = |v_s||i_m| \tag{5.54}$$

$$\lambda_m = 1.5\frac{L_m}{v_s}s_m \tag{5.55}$$

$$\lambda_m = 1.5\frac{L_m}{v_s}|v_s||i_m| = 1.5L_m|i_m| \tag{5.56}$$

Equation (5.55) indicates that the magnetizing flux is not influenced by the choice of voltage space vector, since all the six non-zero voltage vectors produce the same s_m. Hence, the flux cannot directly be controlled by utilizing the information from either active or reactive power.

From equation (5.56), we can see that the magnetizing flux can be controlled by adjusting the magnetizing current $|i_m|$.

$$i_m = i_s + i_r \qquad\qquad (5.57)$$

i_m is the sum of stator current and rotor current, as shown by Equation (5.57). It is know that the stator current is influenced by the stator voltage and the rotor current depends on the load condition and kinetic characteristics which are usually constant. Therefore, we can simply control the stator current to control the flux.

5.4 Simulations

A simple way to observe power distribution in the induction motor is to analyze the powers produced by the DTC. Here the DTC is simulated using Matlab. The motor parameters are listed in the APPENDIX. The reference mechanical speed ramps up to $110\ rad/sec$ at 0.6 s, then kept constant. The load torque is zero before 1.0 s and jumps up to $60\ N.m$ at 1.0 s. The torque band limit is $0.01\ N.m$ The reference stator flux is $0.7\ Wb$, the stator flux band limit is $0.005\ Wb$. The DC voltage for the inverter is 330 V, and the simulation step is $20\ \mu s$.

Figures 5.2 and 5.3 show the mechanical speed and electromagnetic torque of the induction motor when DTC is employed. Figure 5.4 shows the total instantaneous active power.
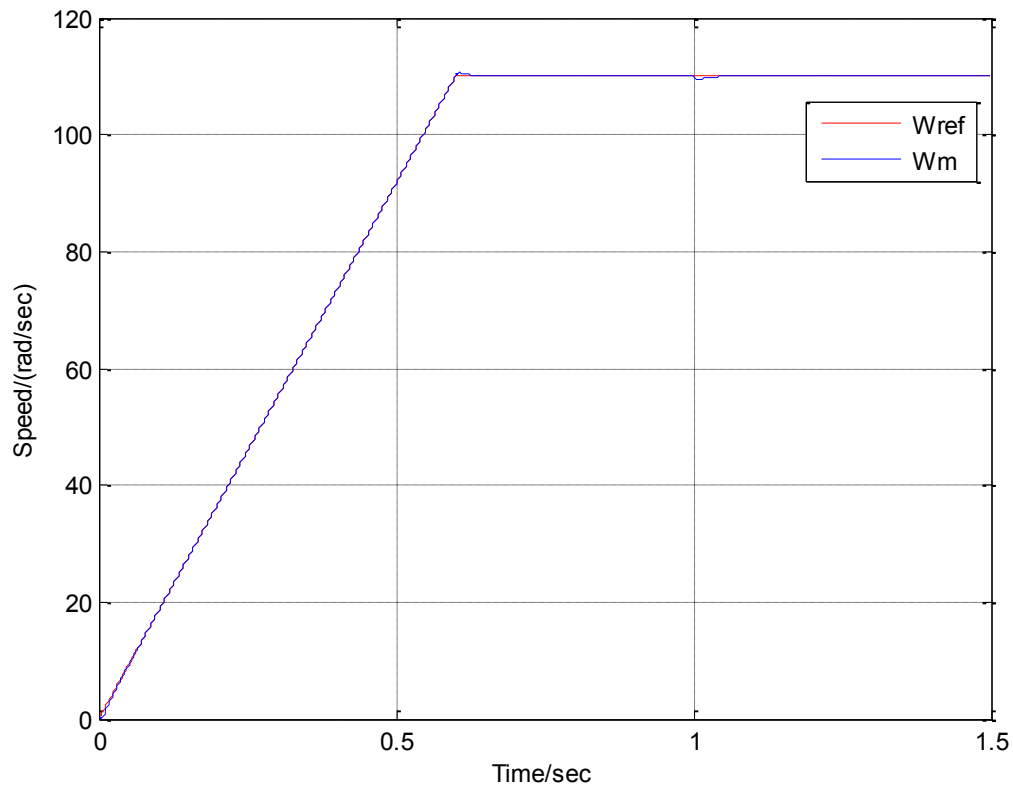

Fig. 5.2 Reference and actual mechanical speeds.
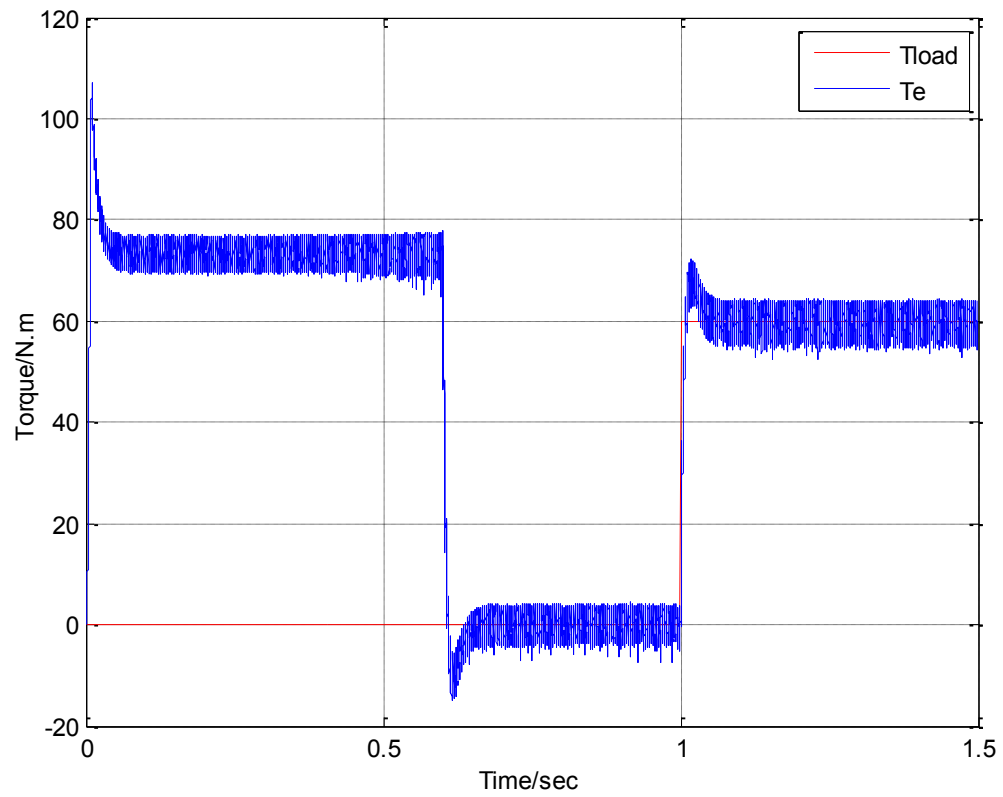
Fig. 5.3 Load torque and electromagnetic torque.
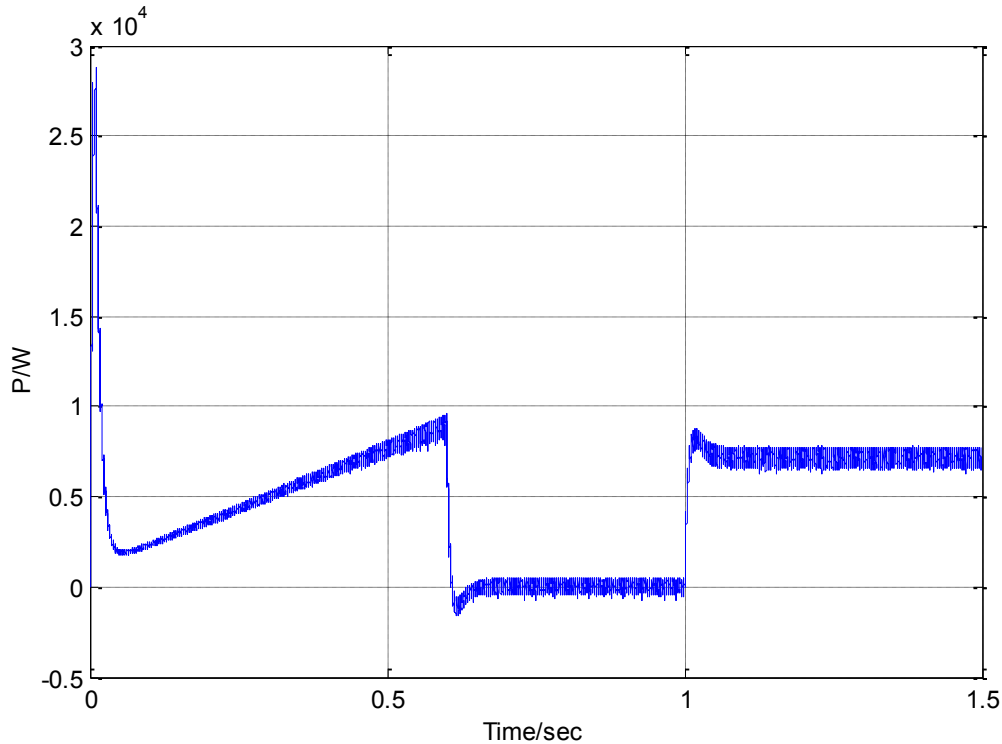
Fig. 5.4 Input active power.

The subsequent simulations are based on the idea that torque can be controlled by adjusting the input active power and the stator flux can be controlled by adjusting the stator current. The later can, in turn, be adjusted through its relationship with the stator voltage vector, such an idea is named as Direct Active Power and Flux Control (DPC).

The $20 - \mu s$ simulation step is very short, compared to the 0.0167 s voltage-source period, so the stator current within can be assumed constant within each simulation step. Six non-zero vectors utilize the same current to get active power based on Table 5.1. The selected voltage vector at $t_{sw} * k_{th}$ s will work during the time interval of $[\, t_{sw} * k_{th},\ t_{sw} * k + 1_{th})$.

The control method of the induction motor switches from DTC to IPC at 1.3 s. Simulation results for the stator flux, mechanical speed, electromagnetic torque, input active power, active powers for six non-zero voltage vectors, stator current, and magnetizing current at and after 1.3 s are summarized in Table 5.2.

Table 5.2. Motor data at 1.3 s

Time/s	FSANG	Fs	Te	ISA	ISANG	IMA	IMANG
1.3	330.36	0.6973	63.88	48.72	40.45	16.52	-35.05
	P_IN	P_1	P_2	P_3	P_4	P_5	P_6
	9955.47	8038.90	9955.47	1916.58	-8038.90	-9955.47	-1916.58

From Table 5.2, the stator flux error is $0.027\,\mathrm{Wb}$ which places it within the flux band, while the torque error $-3.88\,\mathrm{N.m}$ is much bigger than the torque band limit of $0.01\,\mathrm{N.m}$, Therefore, the torque must to be decreased and the stator flux need not be changed.

From the DTC principle, it is known that the zero-vectors do not change the stator flux but decrease the torque. Therefore, the zero-vector was tried during the time interval of 1.3 s to 1.30002 s. The updated data obtained at 1.30002 is given in Table 5.3. The decrease of input power from $9955.47\,\mathrm{W}$ to zero leads to the decrease of torque from $63.88\,\mathrm{N.m}$ to $60.69\,\mathrm{N.m}$; Zero vector causes the decrease of stator current from $48.47\,\mathrm{A}$ to $46.45\,\mathrm{A}$, which leads the decrease of stator flux drops from $0.6973\,\mathrm{Wb}$ to $0.6972\,\mathrm{Wb}$. Thus, the zero vector can be selected at 1.3 s to control the motor.

Table 5.3. Motor data at 1.30002 s with zero vector

Time/s	FSANG	Fs	Te	ISA	ISANG	IMA	IMANG

1.30002	330.36	0.6972	60.69	46.45	39.89	16.52	-34.80
	P_IN	P_1	P_2	P_3	P_4	P_5	P_6
	0.00	7727.30	9457.71	1730.41	-7727.30	-9457.71	-1730.41

As an alternative choice, the vector V_{100} is considered. From Table 5.2, the stator current position is $40.45\,°$, V_{100} provides positive d-q components in the stationary reference frame, so it can increase the stator current slightly. Meanwhile, its corresponding active power is 8038.90 W which is less than the input power of 9955.47 W. Therefore, V_{100} should increase the stator flux and decrease the torque. Table 5.4 shows the relevant data at 1.30002 s with V_{100} during time interval of 1.3 s to 1.30002 s.

Table 5.4. Motor data at 1.30002 s with V_{100}

Time/s	FSANG	Fs	Te	ISA	ISANG	IMA	IMANG
1.30002	330.60	0.7029	63.22	48.88	37.55	16.56	-34.70
	P_IN	P_1	P_2	P_3	P_4	P_5	P_6
	8402.83	8402.83	9795.48	1392.65	-8402.83	-9795.48	-1392.65

Comparing Tables 5.2 and 5.4, it can be seen that the flux increases and torque decreases. Here the V_{100} was selected for the analysis of the impact of non-zero vectors on the flux.

From Table 5.4, the flux error is 0.0029 Wb and torque error is -3.22 N.m, so the flux is still acceptable and the torque must be decreased. The input active power is 8402.83 W. Vector V_{010} has lower active power, 1392.65 W, thus it is selected to lower the torque. It

has a negative *d* component and a positive *q* component, and its relative position to the stator current is $82.45\,°$, so it will lower the stator current slightly. Table 5.5 shows the new data at 1.30004 s.

Table 5.5. Motor data at 1.30004 s with V_{010}

Time/s	FSANG	Fs	Te	ISA	ISANG	IMA	IMANG
1.30004	330.85	0.6972	61.63	47.11	40.61	16.52	-34.37
	P_IN	P_1	P_2	P_3	P_4	P_5	P_6
	1881.36	7754.42	9635.78	1881.36	-7754.42	-9635.78	-1881.36

Comparing Tables 5.4 and 5.5, we see that both the flux and torque decrease, as expected. The flux error is $0.028\,\mathrm{Wb}$ and the torque error is $-1.63\,\mathrm{N.\,m}$. Still the flux is acceptable and torque must be decreased. Observe the powers for non-zero vectors, vector V_{010} is selected for the time interval of 1.30004 s to 1.30006 s. The corresponding results are given in Table 5.6,

Table 5.6. Motor data at 1.30006 s with V_{010}

Time/s	FSANG	Fs	Te	ISA	ISANG	IMA	IMANG
1.30006	331.11	0.6915	60.09	45.49	43.87	16.47	-34.04
	P_IN	P_1	P_2	P_3	P_4	P_5	P_6
	2365.12	7111.29	9476.41	2365.12	-7111.29	-9476.41	-2365.12

From Table 5.6, we can see that both the flux and torque decrease, which confirms the expectation. Now the flux error is $0.0085\,\mathrm{Wb}$ and torque error is $-0.09\,\mathrm{N.\,m}$, so that the stator flux must be increased and the torque must be decreased. If we employ the

vector V_{010}, both the stator flux and torque decrease, as shown in Table 5.7, because V_{010} generates a negative d-component voltage and a low active power.

Table 5.7. Motor data at 1.30008 s with V_{010}

Time/s	FSANG	Fs	Te	ISA	ISANG	IMA	IMANG
1.30006	331.37	0.6859	58.61	44.04	47.33	16.43	-33.71
	P_IN	P_1	P_2	P_3	P_4	P_5	P_6
	2843.96	6473.41	9317.38	2843.96	-6473.41	-9317.38	-2843.96

If we select V_{100}, the flux will increase and torque will decrease, since it has a positive d-component voltage, and its active power is much higher than the input power in Table 5.6. Table 5.8 shows the data for 1.30008 s with V_{100}. The results show that the flux increases while the torque decreases. Now the flux error is 0.029 Wb and the torque error is 0.6 N. m.

Table 5.8. Motor data at 1.30008 s with V_{010}

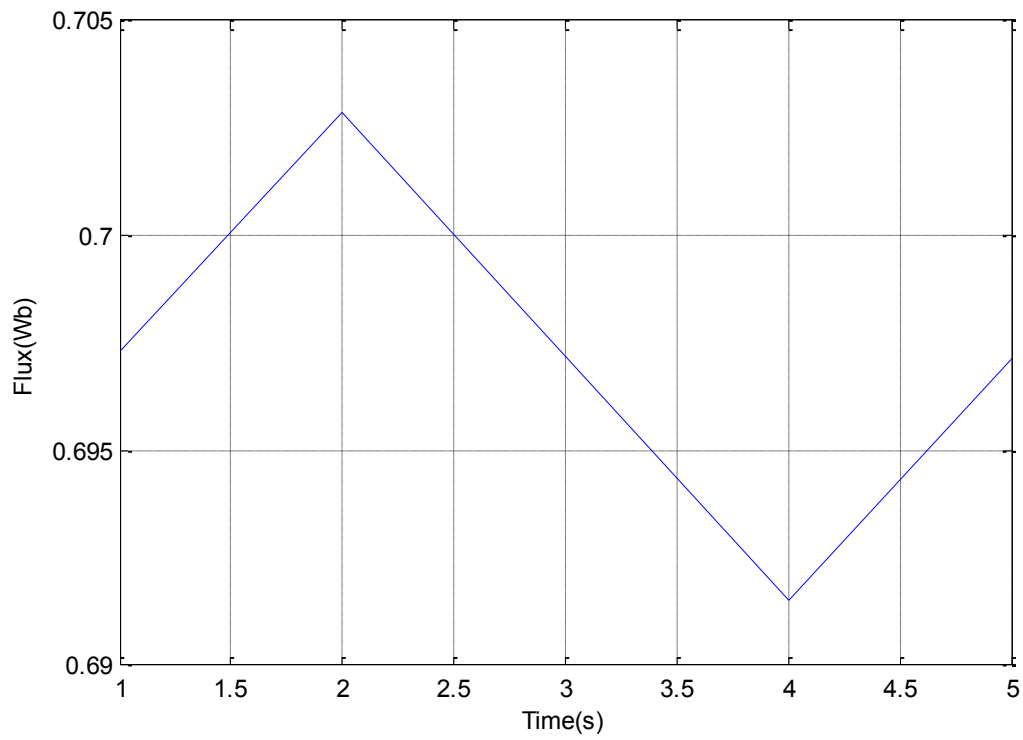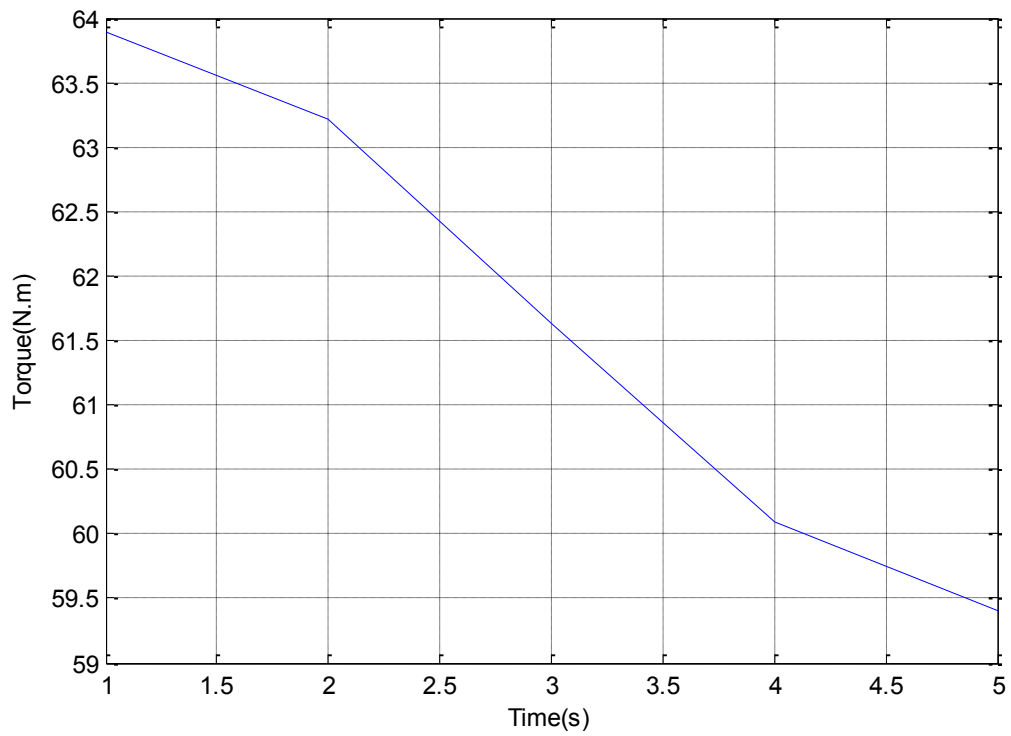| Time/s	FSANG	Fs	Te	ISA	ISANG	IMA	IMANG
1.30006	331.35	0.6971	59.40	45.53	40.69	16.52	-33.69
	P_IN	P_1	P_2	P_3	P_4	P_5	P_6
	7486.70	7486.70	9317.38	1830.67	-7486.70	-9317.38	-1830.67

Fig. 5.5 Stator flux.
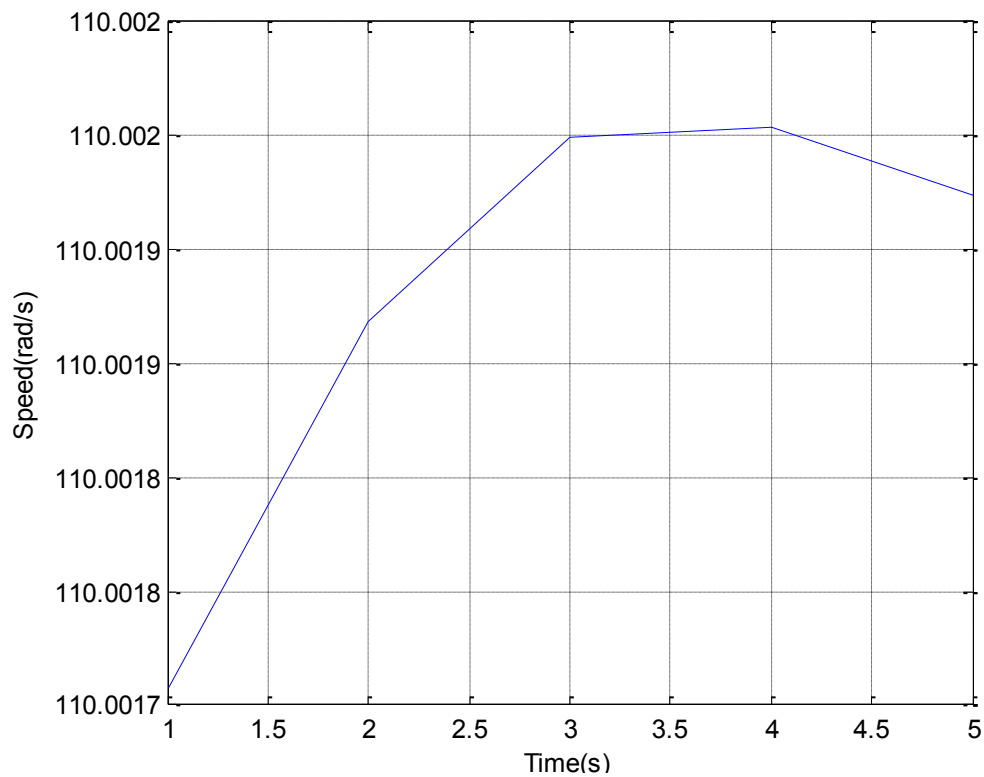
Fig. 5.6 Electromagnetic torque.

Fig. 5.7 Mechanical speed.

Figure 5.5 shows the flux waveform between 1.3 s and 1.30008 s. Figures 5.6 and 5.7 show the corresponding torque and mechanical speed.   The results show that all waveforms are acceptable.

From the above analysis, it can be concluded that the stator flux can be controlled by adjusting the stator current, and the torque can be controlled by adjusting the input active power.

5.5 Conclusion

Based on *p-q* theory, the active and reactive power for each voltage space vector were analyzed. Further, the instantaneous power distribution in the motor was analyzed to determine relationships between the torque, flux, and instantaneous powers. The simplified model of the induction motor and its power distribution were also analyzed. The analysis shows that the torque can be controlled by adjusting the input active power, and flux can be controlled by adjusting the stator current using a suitable voltage space vector. These conclusions were confirmed by simulations.

CHAPTER 6

SENSORLESS INSTANTANEOUS POWER CONTROL OF INDUCTION MOTORS

Instantaneous power control of an induction motor was first proposed by Betz in [31]. It was based on the control of the instantaneous real and imaginary power supplied to the machine. It exploited the fact that the real power minus losses produces the torque produced by the machine, and the imaginary power is needed for the magnetic flux. Conceptually IPC lies between field oriented control (FOC) and direct torque control (DTC). As in DTC, the induction motor model can be implemented in the stationary reference frame. As in FOC, the stator current is split into a real-power current and an imaginary power current in order to control the electromagnetic torque and stator flux separately. After Betz, Lee proposed sensorless IPC for induction motors fed by a three-phase matrix converter. To improve the low-speed sensorless performance, the nonlinear features of the matrix converter, such as commutation delays, turn-on and turn-off times of switching devices, and on-state device voltage drop were modeled using a PQ-power transformation and compensated using a modified reference power. In this chapter, an improved sensorless IPC scheme is presented.

6.1 Instantaneous Active and Reactive Power

From Equations (5.1) and (5.2), the instantaneous active and reactive power for the induction motor can be defined as,

$$p = \frac{2}{3}\left(v_d i_d + v_q i_q\right) \tag{6.1}$$

$$q = \frac{2}{3}\left(v_q i_d - v_d i_q\right) \tag{6.2}$$

6.2 Power Reference Generation

From Chapter 4, we know that the input active power is related to the slip frequency through what is known as slip power. In [44] the author utilizes the difference between reference mechanical speed and speed to compensate for the slip power. In [39-40] the author uses the reference torque to compensate for the slip power. In the synchronous reference frame with the *D*-axis (Q-axis) oriented with air-gap flux vector, the imaginary power is related to the *Q*-axis stator current, the real power is related to the *P*-axis current, as we can see from Figure 6.1.
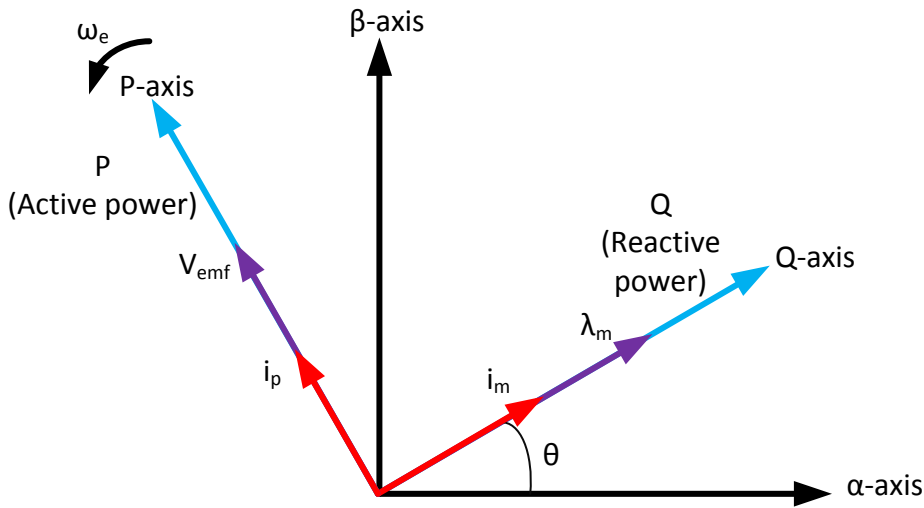

Fig. 6.1 Space vector diagram for power control.

From Chapter 3, we have

$$\omega_{sl} = s\omega_b = \frac{i_{qa}}{\frac{\lambda_{ma}}{L_m}\tau_r} = \frac{i_{qa}}{i_{da}\tau_r} \tag{6.3}$$

$$T_e = \frac{2}{3}p_p i_{qa} i_{da} L_m = \frac{2}{3}p_p i_{qa}\lambda_m \tag{6.4}$$

Therefore, we can get the reference slip frequency:

$$\omega_{sl}{}^* = \frac{3T_e^*}{2p_p i_{da} \lambda_m{}^* \tau_r}$$
(6.5)

The reactive power reference can be expressed as,

$$Q^* = i_m(\omega_{sl}{}^* + \omega_r)\lambda_m^* = \frac{\lambda_m^{*}{}^2}{L_m}\omega_r + \frac{3T_e^*}{2p_p \tau_r}$$
(6.6)

The active power reference is,

$$P^* = \frac{Q^* T_e^* L_m}{p_p \lambda_m^{*}{}^2}$$
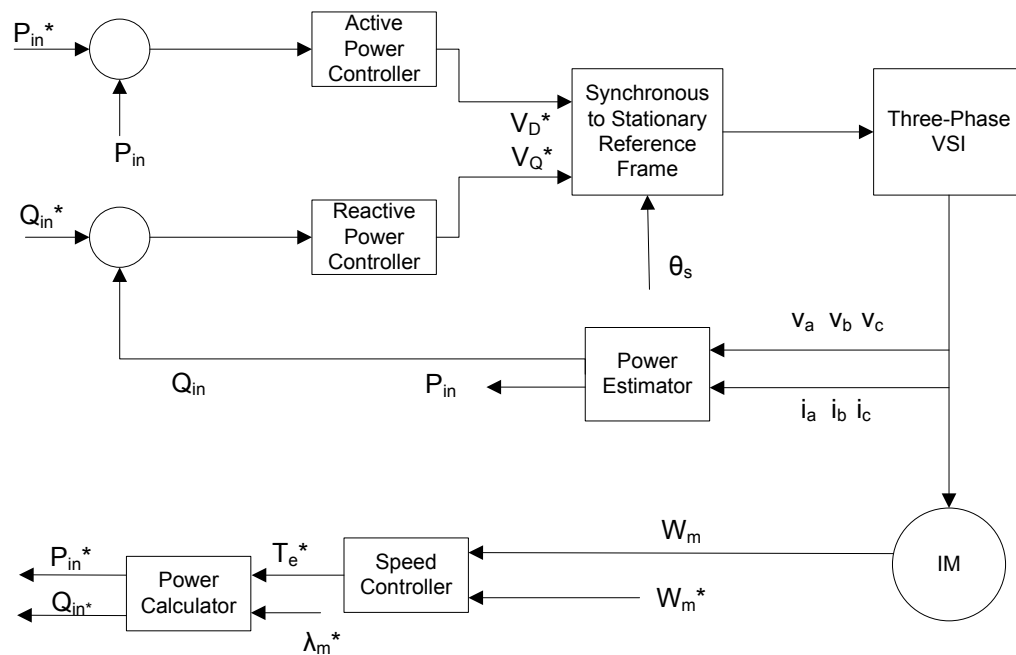(6.7)

Fig. 6.2 Block diagram of instantaneous power control of induction motor.

Figure 6.2 shows the schematic of original IPC, the rotor mechanical speed comes from the induction motor directly.
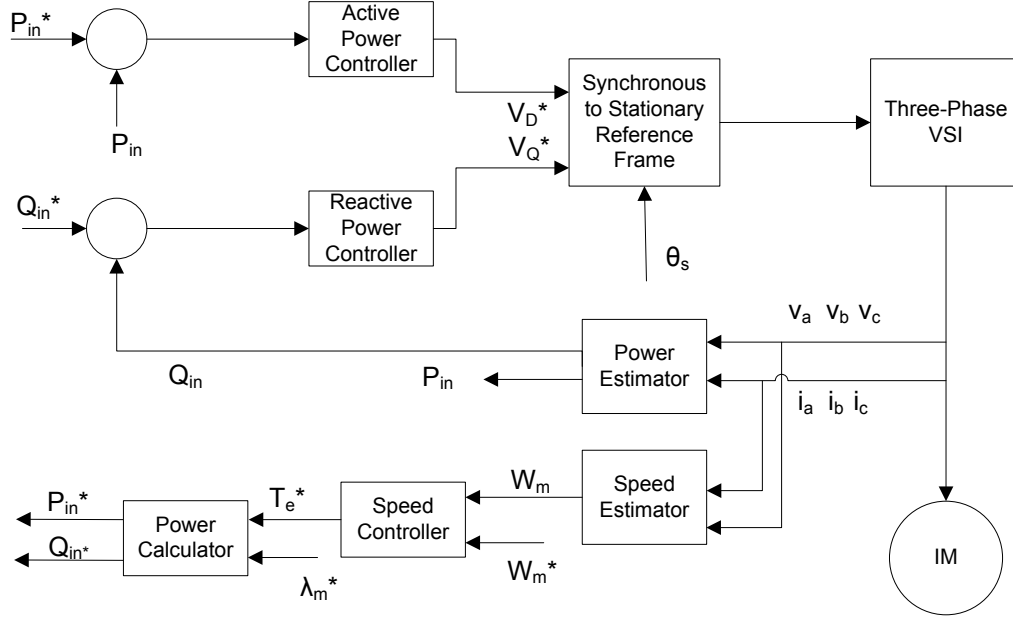
Fig. 6.3 Block diagram of sensorless instantaneous power control of induction motor.

Sensorless estimation of rotor speed is analyzed next. In [49] five sensorless schemes are presented for the estimation of rotor speed. In the IPC of induction motor, the fourth is adopted, and it uses the euqation

$$\omega_r = w_s - \omega_{sl} = (\lambda_{dr} \frac{d\lambda_{qr}}{dt} - \lambda_{qr} \frac{d\lambda_{dr}}{dt})/|\lambda_r|^2$$

$$-\frac{L_m}{\tau_r |\lambda_r|^2}(\lambda_{dr} i_{qs} - \lambda_{qr} i_{ds}) \qquad (6.8)$$

$$\lambda_{dr} = \lambda_{dm} + L_{lr} i_{dr} \qquad (6.9)$$

$$\lambda_{qr} = \lambda_{qm} + L_{lr} i_{qr} \qquad (6.10)$$

$$i_{dr} = \frac{\lambda_{dm}}{L_m} - i_{ds} \qquad (6.11)$$

$$i_{qr} = \frac{\lambda_{qm}}{L_m} - i_{qs} \qquad (6.12)$$

Once we get an estimate of the rotor speed, the ω_r in Equation (6.6) can be replaced with Equation (6.8) to obtain the imaginary power reference, thus forming a close loop control system.

There are three PI controllers in the driving system, including the speed PI controller. To simplify the PI controller adjustment, first adjust the speed PI controller to make it work for the DTC. Since we use the same torque reference in both DTC and IPC, this PI controller also works for IPC. Then we adjust the other two PI controllers. The stator voltage in synchronous reference can be obtained from the transformation from synchronous to stationary reference frame, as seen from Figure 6.3.

6.3 Simulation Test

The simulation presented in this section use the motor given in APPENDIX. The reference air-gap flux is $0.68\,Wb$, the reference mechanical speed and load torque profile is given in Figures 6.4 and 6.5 separately. At 0.8 s, the control method switches from DTC to IPC. The reason why DTC is applied to the induction motor drive system is to build up the flux magnetic field. First, the original instantaneous power control was simulated.
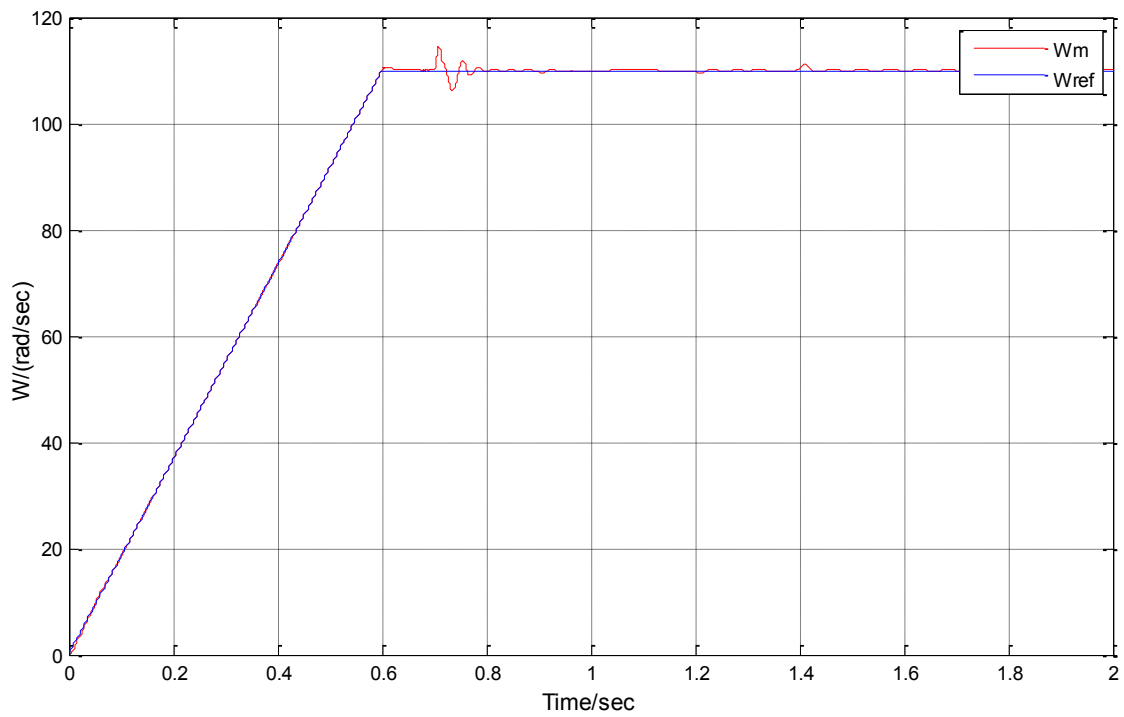
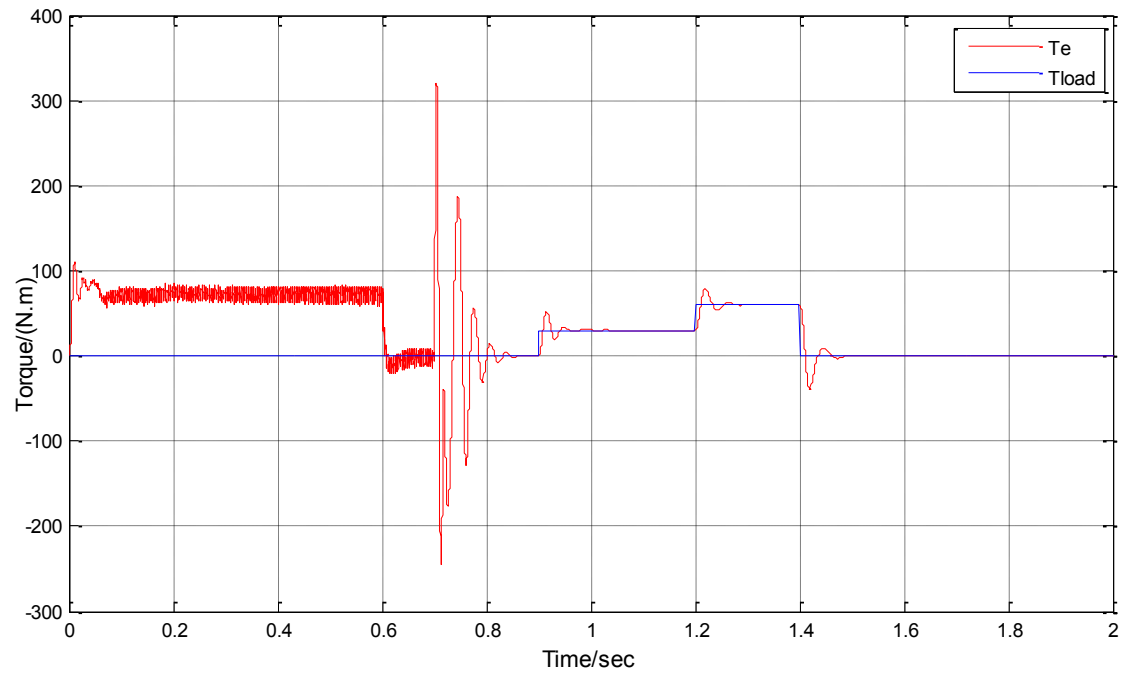Fig. 6.4 Reference and actual speeds.

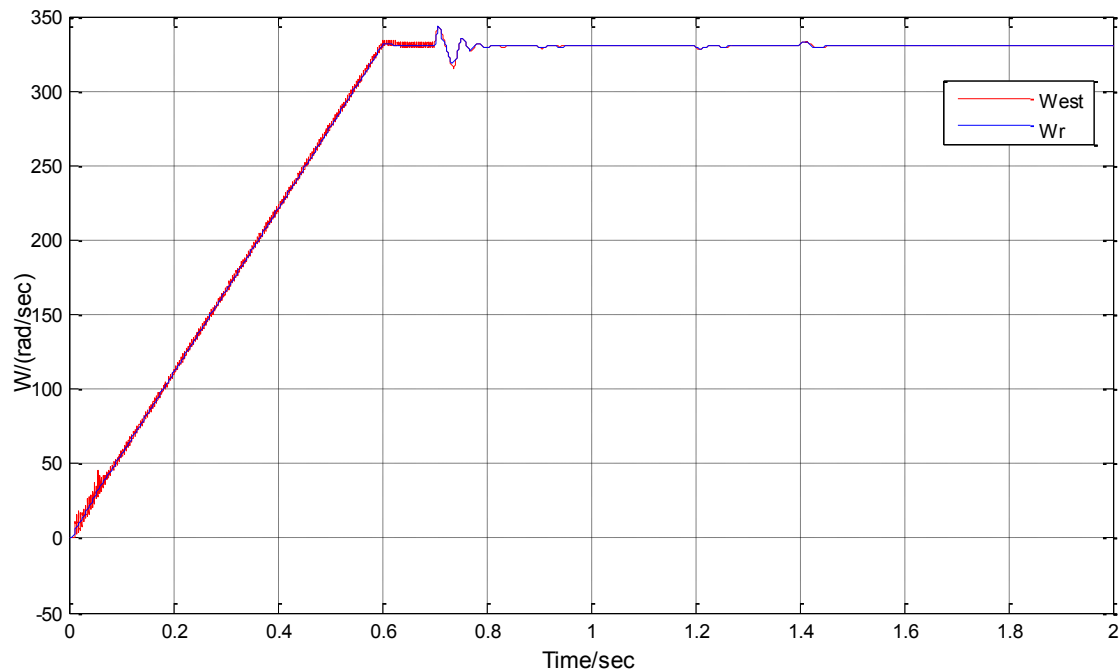Fig. 6.5 Electromagnetic torque and load torque.

Fig. 6.6 Estimated and actual speeds.

From Figures 6.4 and 6.5, we observe that instantaneous power control works well both in the steady and transient states. Figure 6.6 shows the estimated rotor speed and actual speed. They coincide well, except in the range where the speed is almost zero.

In the next step, the estimated speed was employed in the control loop, as shown by Figure 6.3. The corresponding simulation results are given in Figures 6.7-6.9. Figure 6.7 shows that the estimated speed tracks the reference one well except at 0.7 s when the control method is switched from DTC to IPC. The speed estimation error is almost zero, as we can see from Figure 6.8. The electromagnetic torque has a good dynamic response during both the steady and transient states.
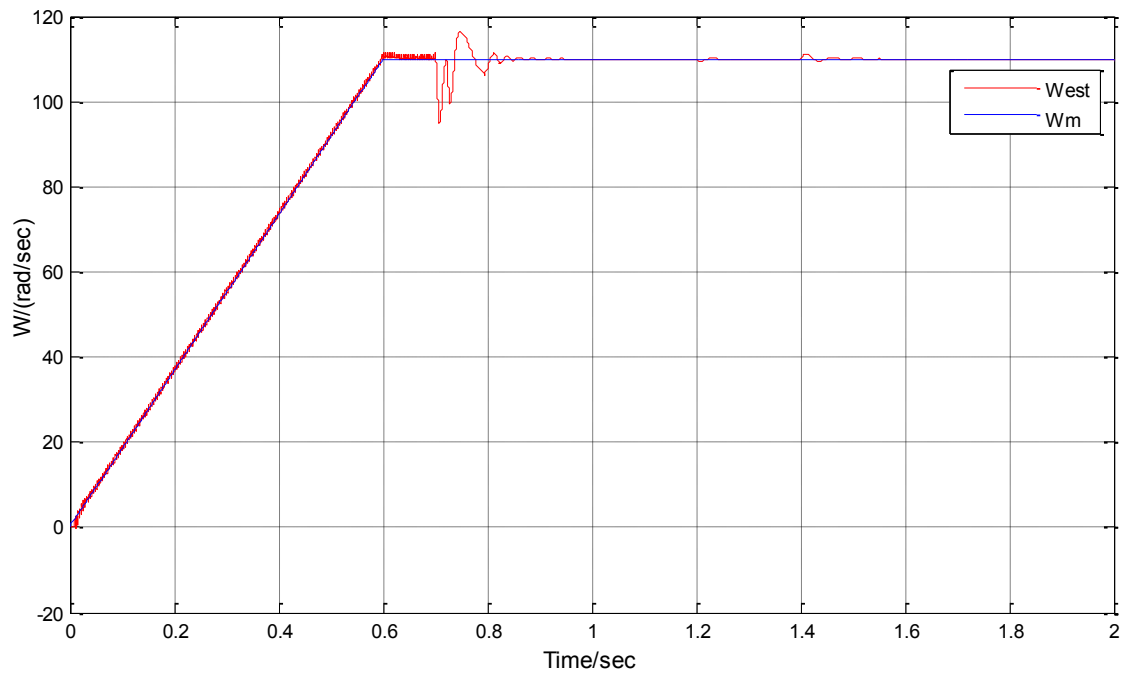
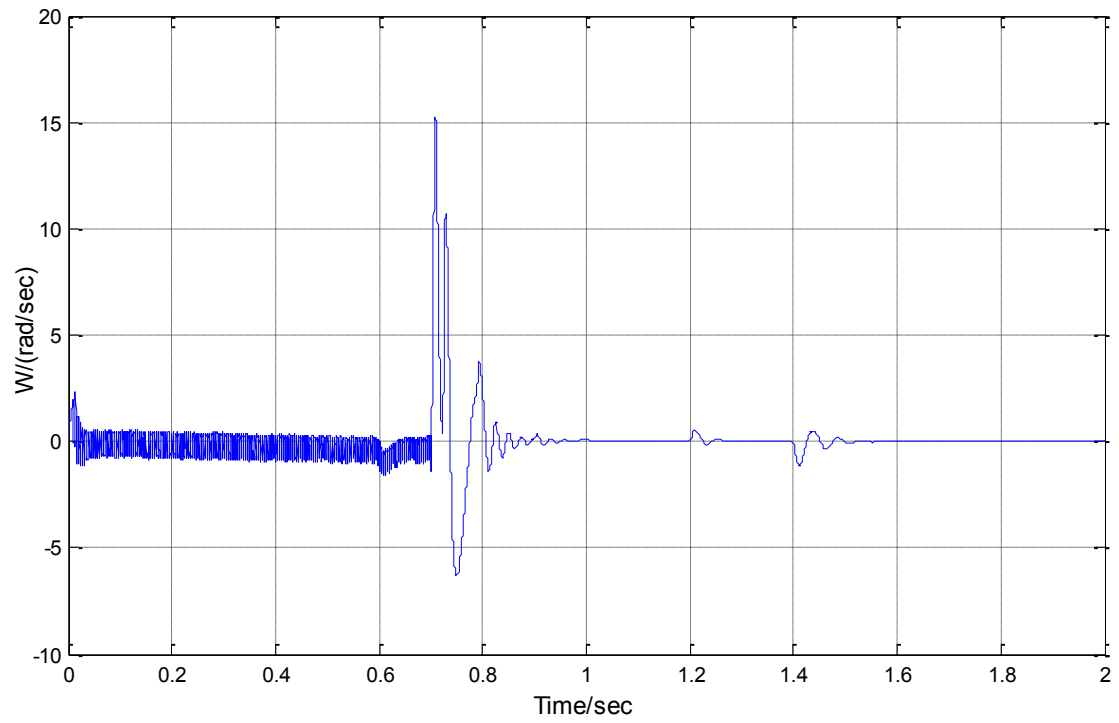Fig. 6.7 Reference and estimated speeds.

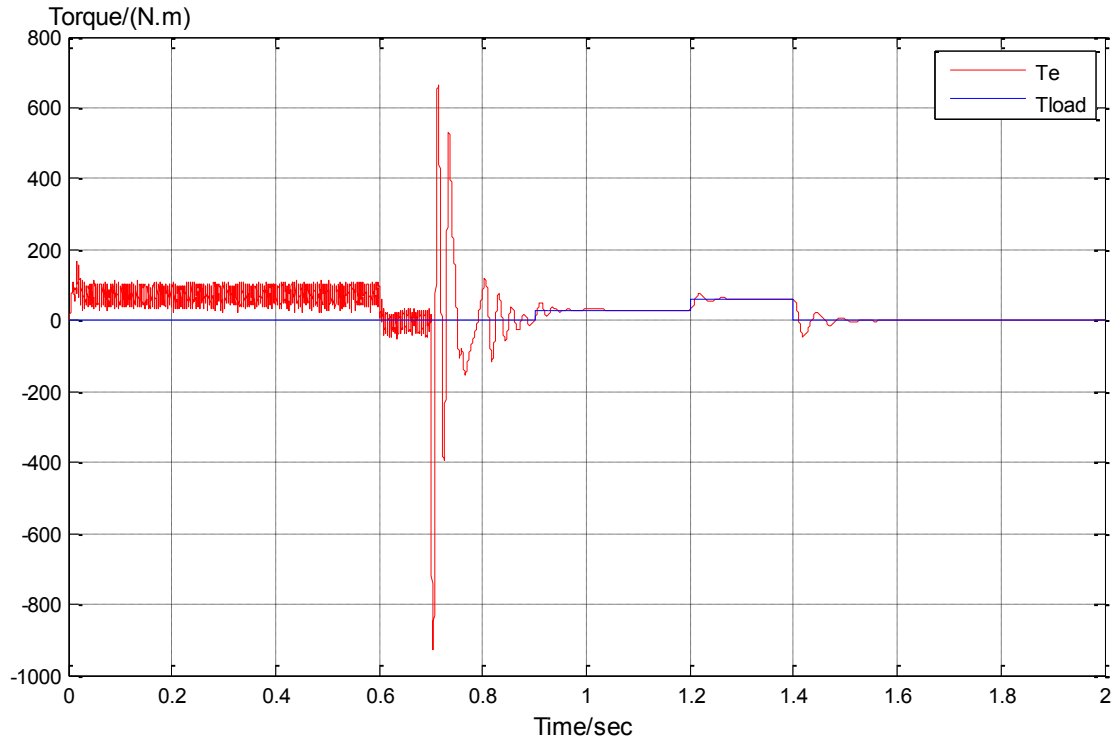Fig. 6.8 Speed estimation error.

Fig. 6.9 Electromagnetic torque and load torque.

6.4 Conclusion

The conventional instantaneous power control of induction motor was presented first, and then a novel sensorless IPC technique was introduced. The simulation results show that the new method works both in the steady and transient states.

CHAPTER 7

CONCLUSION

The performed analysis and simulations has shown that the reactive power cannot directly control the magnetic flux of induction motor. Instead, the flux can be controlled by adjusting the stator current using a suitable voltage space vector. The torque can be controlled by adjusting the input active power. We call this method direct power control (DPC).

Assuming that the stator current does not change significantly in the course of a switching cycle, input active powers for all six non-zero vectors were calculated. Based on the torque and flux error, suitable voltage vectors were considered for selection for the next cycle by comparing the needed active power with those generated by non-zero inverter states, and analyzing the relative position of corresponding voltage vector to stator current vector. The simulations have confirmed validity of the DPC.

A novel sensorless IPC technique, which is an expansion of the known method, was proposed. It has been shown that the IPC needs some other control technique, such as the DTC, to establish the required flux level when the machine starts. The sensorless IPC provides a good dynamic response.

REFERENCES

[1] A. M. Trzynadlowski, "The Field Orientation Principle in Control of Induction Motors," *Kluwer Academic Publishers*, Boston, 1994.

[2] T. Irisa, S. Takaka, R. Ueda, and T. Sonoda, "On reliability of induction machine for high performance based on parameter characteristics," Conf. Rec. IEEE-IAS Annual Mtg., 1983, pp. 547-554.

[3] R. Ueda, T. Sonoda, K. Fujitani, Y. Yoshida, and T. Irisa, "Investigation of Induction motor characteristics by means of vector control," Conf. Rec. IEEE-IAS Annual Mtg., 1985, pp.578-585.

[4] A. Schwery, B. Kawkabani, J. J. Simond, and A. Elmaleh, "A stator flux oriented vector control for induction motor drives," Swiss Federal Institute of Technology, Warner Electric S. A. Switzerland.

[5] G. Liu, and J. Lu, "A stator flux-oriented decoupling control scheme for induction motor," Conf. Rec. IEEE Intl. Conf. on Control and Automation, Guangzhou, China, 2007, pp. 1701-1704.

[6] R. De Doncker, and D. W. Novotny, "The universal field oriented controller," Conf. Rec. IEEE-IAS Annual Mtg., 1988, vol.1, pp. 450-456.

[7] R. De Doncker, and F. Profumo, "The universal field oriented controller applied to tapped stator windings induction motors," Conf. Rec. IEEE-PESC'89, 1989, Milwaukee, vol.2, pp. 1031-1036.

[8] R. De Doncker, F. Profumo, and A. Tenconi, "The universal field oriented (UFO) controller in the air-gap reference frame," Conf. Rec. PESC '90, 1990, Tokyo, Japan, pp. 61-68.

[9] R. De Doncker, F. Profumo, and M. Pastorelli, "Self tuning of induction motor servo drives using the universal field oriented controller," Conf. Rec. IEEE-PESC '90, San Antonio, June 1990, pp. 649-655.

[10] F. Profumo, R. De Doncker, and A. Tenconi, "The universal field oriented (UFO) controller applied to a wide speed range induction motor drives," Conf. Rec. PESC '91, Boston (USA), June 1991, pp. 681-686.

[11] R. De Doncker, F. Profumo, M. Pastorelli, and P. Ferraris, "Comparison of universal field oriented (UFO) controllers in different reference frames," IEEE Trans. on Power Electronics, 1995, vol. 10, no. 2, pp. 205-213.

[12] I. Takashi, T. Noguchi, "A new quick-response and high-efficiency control of an induction motor," IEEE Trans. Industry Applications, 1986, vol. 22, no.5, pp. 820-827.

[13] M. Depenbrock, "Direct self-control (DSC) of inverter-fed induction machines," IEEE Trans. Power Electronics, 1988, vol. 3, no. 4, pp. 420-429.

[14] H. R. Keyhani, M. R. Zolghadri, A. Homaifar, "An extended and improved discrete space vector modulation direct torque control for induction motors," Conf. Rec. 35th Annual IEEE Power Electronics Specialists Conf., Germany, 2004, pp. 3414-3420.

[15] R. H. Ahmad, G. G. Karady, T. D. Blake, and P. Pinewski, "Comparison of space vector modulation techniques based on performance indexes and hardware implementation," Conf. Rec. 23rd Intl. Conf. on Industrial Electronics, Control and Instrumentation, IECON 97, vol. 2, pp. 682-687.

[16] E. Ozkop, and H. I. Okumus, "Direct torque control of induction motor using space vector modulation (SVM-DTC)," Conf. Rec. 12th Intl. Middle-East Power System Conf., 2008, pp. 368-372.

[17] T. Habetler, F. Profumo, M. Pastorelli, and L. Tolbert, "Direct torque control of induction machines using space vector modulation", IEEE Trans. on Ind. Appl., 1992, vol.28, no.5, pp. 1045-1053.

[18] A. Mortezaei, N. A. Azli, N. R. N. Idris, S. Mahmoodi, and N. M. Nordin, "Direct torque control of induction machines utilizing 3-level cascaded H-bridge multilevel inverter and fuzzy logic," Conf. Rec. APEC, 2011, pp. 116-121.

[19] V. Perelmuter, "Three-level inverters with direct torque control," Conf. Rec. IEEE Industry Application Conf., 2000, vol.3, pp. 1368-1374.

[20] J. Beerten, J. Verveckken, and J. Driesen, "Comparison of three-level torque hysteresis controller for direct torque control, " Conf. Rec. EUROCON 2009, pp. 1950-1955.

[21] X. Del Toro, M. G. Jayne, P. A. Witting, J. Pou, A. Arias, and J. L. Romeral, "New direct torque control scheme for induction motors," Conf. Rec. 2005 European Conf. on Power Electronics and Application, pp. 9 pp. –P.9.

[22] J. Yang, and H. Jin, " Direct torque control system for induction motors with fuzzy speed PI regulator", Conf. Rec. Fourth Intl. Conf. on Machines Learning and Cybernetics ,Guangzhou , 2005, pp.778-783.

[23] H. F. E. Soliman, and M. E. Elbuluk, "Direct torque control of a three phase induction motor using a hybrid PI/fuzzy controller", Conf. Rec. 42nd IEEE IAS Annual Mtg., 2007, pp. 1681-1685.

[24] S. Mir, and M. E. Elbuluk, "Precision torque control in inverter- fed induction machines using fuzzy logic", Conf. Rec. 26th Annual IEEE Power Electronics Specialists Conf., 1995, vol.1, pp. 396-401.

[25] T. Y. Abdalla, H. A. Hairik, and A. M. Dakhil, "Minimization of torque ripples In DTC of induction motor using fuzzy mode duty cycle controller," Conf. Rec. 26th Annual IEEE Conf. on Energy, Power and Control, 2010, pp. 237-244.

[26] A. A. Pujol, "Improvements in direct torque control of induction motor," Master Thesis, University Polytechnic of Catalunya, 2000.

[27] L. Romeral, A. Arias, E. Aldabas, and M. G. Jayne, "Novel direct torque control (DTC) scheme with fuzzy adaptive torque ripple reduction", IEEE Trans. Ind. Electron., vol.50, no.3, pp. 487-492, 2003.

[28] C. Lin, K. -L. Fang, and Z.-F. Hu, "A scheme of fuzzy direct torque control for induction machine," Conf. Rec Fourth Intl. Conf. on Machine Learning and Cybernetics , Guangzhou , 2005, pp.803- 807.

[29] I. G. Bird, and H. Zelaya De La Parra, "Fuzzy logic torque ripple reduction for DTC based AC drives," IEEE Electronics Letters, vol.33, no.17, 1997, pp. 1501-1502.

[30] M. Elbuluk, "Torque ripple minimization in direct torque control of induction machines," Conf. Rec IEEE-IAS Annual Mtg., 2003, pp. 11-16.

[31] R. E. Betz, and B. J. Cook, "Instantaneous power control – an alternative to vector and direct torque control?" Conf. Rec. of IEEE-IAS Annual Mtg., 2000, pp. 1640-1647.

[32] R. E. Betz, S. Henriksen, B. J. Cook, and T. Summers, "Practical aspects of instantaneous power control of induction machines," Conf. Rec. IEEE-IAS Annual Mtg., 2001, vol.3, pp.1771-1778.

[33] R. E. Betz, and B. J. Cook, "Instantaneous power control of induction machines," Department of Electrical and Computer Engineering, University of Newcaste, Australia, Tech. Rep. EE00022, 2000.

[34] R. E. Betz, and T. Summers, "Sensorless instantaneous power control of induction machines," Conf. Rec. 2005 European Conf. on Power Electronics and Applications, pp. 10-17.

[35] R. E. Betz, and T. Summers, "Speed estimation of induction machines using imaginary power," Conf. Rec. IEEE-IAS Annual Mtg., 2003, pp. 117-123.

[36] T. Summers, and R. E. Betz, "Instantaneous power control of induction machines using a novel filtering approach on the back-EMF estimates," Conf. Rec. Second Intl. Conf. on Power Electronics,, Machines and Drives, 2004, vol.1, no.498, pp. 314-319.

[37] T. Summers, and R. E. Betz, "Stability analysis of the instantaneous power control (IPC) algorithm for induction machines," Conf. Rec. European Conf. on Power Electronics and Applications, 2007, pp. 1-10.

[38] R. Datta, and V. T. Ranganathan, "Direct power control of grid-connected wound rotor induction machine without rotor position sensors," IEEE Trans. on Power Electronics, 2001, vol.16, pp. 390-399.

[39] K.-B. Lee, and F. Blaabjerg, "Sensorless power control for induction motor drives fed by a matrix converter," Conf. Rec. IEEE-IAS Annual Mtg., 2006, vol.3, pp. 1242-1248.

[40] K.-B. Lee, and F. Blaabjerg, "Simple power control for sensorless induction motor drives fed by a matrix converter," IEEE Trans. on Energy Conversion, vol. 23, pp. 781-788.

[41] M. Malinowski, M. P. Kazmierkowski, and A. M. Trzynadlowski, "Direct power control of virtual flux estimation for three-phase PWM rectifiers," Conf. Rec. 2000 IEEE Intl. Symp. on Industrial Electronics, vol. 2, pp. 442-447.

[42] M. Malinowski, M. P. Kazmierkowski, and A. M. Trzynadlowski, "A comparative study of control techniques for PWM rectifiers in AC adjustable speed drives," IEEE Trans. on Power Electronics, 2003, vol.18, no. 6, pp. 1390-1396.

[43] M. Jasinski, P. Antoniewicz, and M. P. Kazmierkowski, "Vector control of PWM rectifier – inverter fed induction machines – a comparison," Conf. Rec. IEEE Conf. on Compatibility in Power Electronics, 2005, pp. 91-95.

[44] X. Luo, "Direct Power Control of Induction Motor," University of Nevada, Reno.

[44] M. Malinowski, and M. P. Kazmierkowski, "Direct power control of three-phase PWM rectifier using space vector modulation – simulation theory," Conf. Rec. IEEE Intl. Symp. on Industrial Electronics, 2002, pp. 1114-1117.

[45] J. Restrepo, J. Viola, M. Aller, and A. Bueno, "A simple switch selection state for SVM direct power control," Conf. Rec. IEEE Intl. Symp. on Industrial Electronics, 2006, pp. 1112-1116.

[46] J. B. G. Manel, A. Jihen, and S. B. Ilhem, "A novel approach of direct active and reactive power control allowing the connection of the DFIG to the grid," Conf. Rec. 13th European Conf. on Power Electronics and Applications, 2009, pp. 1-10.

[47] Ion Boldea, and S. A. Nasar, "Electric Drives," Taylor & Francis Group, 2006.

[48] H. Akagi, E. H. Watanade, and M. Aredes, "Instantaneous Power Theory and Applications to Power Conditioning," WILEY – INTERSCIENCE, 2007.

[49] Peter Vas, "Sensorless Vector and Torque Control," Oxford University Press, 1998.

APPENDIX

Characteristics of the example induction motor

The example motor used in the simulations is a 10 hp three-phase squirrel-cage induction motor. Detailed specification of the motor are listed in table A.1 [1].

Table A.1. Parameters of the example induction motor

Parameter symbols		
Rated Power	P_{rat}	10 hp
Rated stator voltage	V_{rat}	230 V/ph
Rated stator current	I_{rat}	39.5 A/ph
Rated frequency	f_{rat}	60 Hz
Rated slip	s_{rat}	0.027
Rated speed	n_{rat}	1168 r/min
Rated torque	T_{rat}	183 N. m
Numbers of Pole pairs	P_p	3
Stator resistance	R_s	0.294 Ω/ph
Stator inductance	L_s	0.0424 H/ph
Rotor resistance	R_r	0.156 Ω/ph
Rotor inductance	L_r	0.0417 H/ph
Magnetizing inductance	L_m	0.041 H/ph
Rotor mass moment of inertia	J_M	0.4 kg. m^2